Results in Materials 23 (2024) 100622

Contents lists available at ScienceDirect

Results in Materials

journal homepage: www.sciencedirect.com/journal/results-in-materials

Chemistry and relevant thermophysical properties of $Pb_{84.3}Li_{15.7}$ liquid solutions: Updated view and identification of new and coherent values

Paolo Favuzza

ENEA, via Madonna del Piano 10, 50019, Sesto Fiorentino (FI), Italy

ARTICLE INFO

Keywords:
Lead-lithium eutectic
Lead-lithium blanket
PbLi
Thermophysical properties
Lorenz number
Sieverts' constant

ABSTRACT

The liquid breeding blanket concept of a fusion reactor is based on the employment of the eutectic Lead-Lithium solution (LLE), where Lithium, enriched in ^{6}Li, has the purpose of regenerating Tritium by reacting with neutrons, while Lead enhances the process acting as neutrons multiplier. Anyway, despite the huge interest on this binary system, LLE is not characterized yet by a fully consolidated description of its basic thermophysical properties and, in many cases, the spread of values reported so far in literature remains still significant. The purpose of this paper is hence to check again the many data available in literature, with a special attention to the ones more recently published, trying to explain and solve their inhomogeneity. Taking into account the general features of the Pb-Li interaction and particularly the not ideal behaviour of the Pb-Li liquid solutions, the following thermophysical properties of the LLE are dealt in detail: specific heat; density and volumetric thermal expansion coefficient; thermal conductivity and diffusivity; electrical resistivity; Sieverts' constant of Hydrogen. Based on the deep analysis of all the reported experimentation and through the adoption of several comparison criteria, the most trustable correlation is sought for each of the above properties; additionally, when a robust correlation couldn't be retrieved, a new, optimized, one has been proposed, capable also to foresee correctly the effect of small composition variations and to assure the internal coherence among linked properties.

Specific heat and density values resulted at the end accurately described and not needing for additional experimentation; thermal properties and electrical resistivity can be evaluated with decent confidence, even if their uncertainty could be somehow reduced by future investigations; for Sieverts' constant it has not possible yet to identify a unique, trustable correlation, anyway the range of values correctly assumed up to 900K has been significantly restricted.

1. Introduction

The capability of Lithium to generate Tritium (^{3}H) when bombarded by a flux of neutrons makes it tremendously attractive for its application as breeder in several, different concepts of fusion reactors currently under investigations. Two conditions are anyway necessary to get its efficient employment in this application: first, since only the isotope 6 of Lithium (^{6}Li) has a sufficiently high cross-section for the reaction with the neutron, Lithium must be enriched in this isotope from its natural abundance of ~7.6 at.% to commonly at least 50 % at.%, depending on the specific type of breeder; second, it is necessary to flank it with a second component acting as neutrons multiplier, to increase the overall yield of the ^{3}H production reaction.

In this regard, several breeder concepts employ Lead as neutron multiplier, hence are based on the whole on the binary Lead-Lithium (Pb-Li[1]) system; according to the specifically selected composition, i.e. the atomic ratio of the 2 metals, and to the phase diagram shown in Fig. 1, there is indeed a large variability in the melting point, and this provides the possibility to hypothesize and study the application of this system both as solid and liquid blanket, at different, properly optimized temperatures. This paper deals with the liquid breeder proposal.

Whether Water Cooled (WC), Helium Cooled (HC) or Dual Cooled (DC), the liquid Pb-Li blanket requires Lithium enriched to ~90 % in ^{6}Li; particularly, the liquid eutectic solution at low Li content (LLE: Li molar fraction ~ 0.157) has been selected for the application, being able to assure a good breeding ratio, permitting to operate down to relatively

E-mail address: paolo.favuzza@enea.it.

[1] Here and henceforward in this paper, the notation Pb-Li (i.e. with the '-' symbol between the chemical elements) will be adopted to describe the generic system or alloy constituted by the two metals, regardless of their atomic ratio, not to generate confusion with LiPb (or PbLi) which denotes instead the specific compound defined by the exact 1:1 stoichiometry.

https://doi.org/10.1016/j.rinma.2024.100622
Received 7 May 2024; Received in revised form 31 July 2024; Accepted 22 August 2024
Available online 27 August 2024

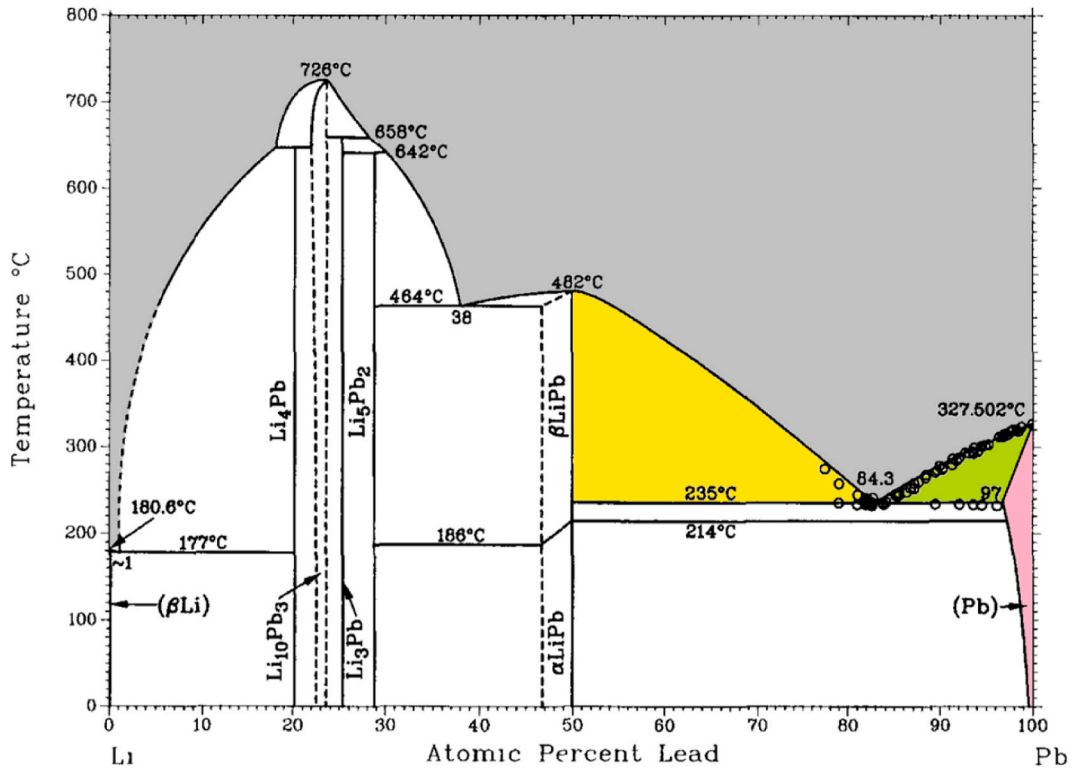

Fig. 1. Phase diagram of the Pb-Li system proposed by Ref. [1]. Circles in the Figure indicate experimental points obtained by Ref. [2].

low temperatures and allowing the easy recovery of generated Tritium from the liquid solution (see section 4.5).

Anyway, despite the huge interest on this binary system, LLE is not a standard system, characterized by a fully consolidated description of its basic thermophysical properties. Many experimentations have been performed since several decades, aiming at determining the correct values of these properties and finding out the proper correlations able to clarify the solution behaviour; anyway, a unique, sure correlation cannot be yet associated to many key parameters and, in some cases, the spread of the experimental values reported in literature by the different authors remains still very significant. The are several possible reasons to explain the encountered inhomogeneity of the data: the different purity level of the investigated solution samples, which follows also from the original purity of the 2 employed metals (Pb and Li) and their significant reactivity, especially in the case of Li, with even the normal atmosphere gases; the nominal composition of the solution actually analysed, which often doesn't correspond exactly to that of the eutectic point, because of the not optimal technique adopted for the preparation of the binary mixture from the single metals (the Pb-Li solution is obtained by melting the solid Pb-Li mixture, which is in turn obtained through different casting processes); above all, the experimental setup, the technique and/or the theoretical modelization adopted for determining the value of a specific property. Furthermore, in some cases no real Pb-Li eutectic solution was directly investigated, but its description was achieved only by extrapolation from solutions characterized by quite different compositions.

The purpose of this article is hence to check the many data available in literature for the eutectic Pb-Li liquid solutions, with a special attention to the ones more recently published, trying to explain and to solve their inhomogeneity. In the first part of the paper, a general overview of the Pb-Li phase system and the many Pb_xLi_y binary compounds will be presented, focussing in particular on the description of the Pb-Li liquid solutions and their theoretical modelization. Then, in the second part, taking also into account the above description, the following thermophysical properties of the eutectic Pb-Li solution will be dealt in detail, searching for a correlation permitting to calculate their values at each desired temperature: specific heat; density; volumetric thermal expansion coefficient; thermal conductivity; thermal diffusivity; Sieverts' constant. In case the data collected in literature will result inconsistent due to the existence of too different correlations for the same parameter, a justified selection of the most appropriate one will be presented or, is some cases, a new, optimized one, will be proposed by elaborating the ensemble of all the available data; in the worst case, in absence of a reliable correlation, a restricted range of trustable values will be at least indicated.

2. The Pb-Li system

2.1. Generalities of the Pb-Li solid compounds

The Pb-Li system, described by the phase diagram in Fig. 1 [1], can be surely defined a not ideal system, due to the possible formation of many different solid intermetallic compounds; to the existence of ranges of temperature/composition values in which 2 or even 3 phases coexist in equilibrium conditions; to the consequent presence of eutectic points; to the liquid phase behaviour (see section 2.3), characterized by mixing excess thermodynamic quantities different from 0.

The Pb-Li composition selected for the liquid breeding blanket (WCLL, HCLL or DCLL) is the one corresponding to the eutectic point located at 235 °C. According to Fig. 1 and to Ref. [2], the corresponding composition results.

- on atomic base: Pb = 84.3 % Li = 15.7 %
- on weight base: Pb = 99.38 % Li = 0.62 %

The heavier metal is therefore in large molar excess respect with the lighter one, and this excess becomes even huge in weight terms. It must not surprise if the temperature of the eutectic (235 °C), which for definition means "*the point where it is easiest to melt*", is indeed higher than pure Lithium one (180.5 °C). In fact, the value of 235 °C is actually a

Table 1
Summary of the main crystallographic data of the many Pb-Li phases (all values at room temperature except for β-LiPb@220 °C)

Phase	Cell Type	Space Group	Cell constants [Å]	Ref.
Li	Cubic (bcc)	Im3m	a = 3.508	[12]
$Li_{22}Pb_5$	Cubic	F23	a = 20.08	[8]
Li_4Pb	Cubic (subcell)		a = 3.34	[8]
Li_7Pb_2	Hexagonal	*P*321	a = 4.751 c = 8.589	[5]
$L_{10}Pb_3$	Cubic	P $\bar{4}$ 3m	a = 10.08	[4]
Li_3Pb	Cubic	Fm3m	a = 6.687	[5]
Li_8Pb_3	Monoclinic	*C2/m*	a = 8.24 b = 4.757 c = 11.03 β = 104.5°	[6]
α-LiPb	Rhombohedral	*R3m*	a = 3.542 α = 89.5°	[7]
β-LiPb	Cubic	Pm3m	a = 3.563	[7]
Pb	Cubic (fcc)	Fm3m	a = 4.950	[13,14]

"local" minimum in the *liquidus* curve of the binary-system, and in this regard, we can see from Fig. 1 that the two solid phases which coexist in the eutectic points are actually pure Pb from one side, and the LiPb intermetallic compound (in its β-structure) from the other. Since pure Pb m.p. is ~327.5 °C and LiPb melting point is ~482 °C, it is easy to verify that 235 °C is a minimum with respect to both the two constituents of the eutectic mixture.

As said, many stable intermetallic Pb-Li compounds are possible in the Li-rich region of the diagram. These compounds, thanks to the strong interaction between the 2 metals, can exist in solid phase with a precisely defined crystalline identity up to relatively high temperature values. Many experimentations and theoretical simulations have been conducted since the first half of the last century in order to characterize the structure of these phases. At first, Grube and Klaiber [3], using thermal and resistometric analysis, presented six intermetallic compounds, i.e. Li_4Pb, Li_7Pb_2, Li_3Pb, Li_5Pb_2, α-LiPb e β-LiPb; Rollier and Arreghini [4] proposed instead the structure for the compound $Li_{10}Pb_3$, corresponding indeed to Li_7Pb_2 described in Ref. [3]; Zalkin [5–8] investigated the crystal structure of $Li_{22}Pb_5$, Li_7Pb_2, Li_3Pb, Li_8Pb_3, α-LiPb e β-LiPb, suggesting that $Li_{22}Pb_5$ was the real crystalline phase in place of Li_4Pb and similarly that Li_8Pb_3 was the real crystalline phase in place of Li_5Pb_2; later Smith and Moser [9] reviewed the entire phase diagram on the basis of [5–7]; Hubberstey [2] gave a relevant contribution particularly in the Pb-rich zone; finally Okamoto [1] presented the phases which are visible in Fig. 1, i.e. Li_4Pb, $Li_{10}Pb_3$, Li_3Pb, Li_5Pb2, α-LiPb e β-LiPb. The crystallographic data of the Lead-Lithium intermetallic compounds collected with time, together with those of pure Pb and Li, are summarized in Table 1.

Particular interest deserves the LiPb 1:1 stoichiometric compound, which is one of the two solid phases formed during the solidification (at 235 °C) of the liquid alloy selected as the liquid blanket. Two different crystalline structures are possible for this LiPb compound: α, which is more stable at lower temperatures, and β, which becomes more stable above 214 °C, including therefore also the eutectic point conditions. The α→β transition at 214 °C was evidenced by the trend of the electrical resistivity of LiPb [7,11], that decreased (anomalously) with temperature approaching the value of 214 °C; at this temperature the slope of the resistivity vs temperature was discontinuous, while, at higher temperature, it became positive.

The crystallographic investigation of β-LiPb also indicates that its structure is similar to that of pure Li, being characterized by the same cell type (cubic) and only a bit higher cell constant, with the Lead atoms replacing the Lithium ones in the centre of the cell body. Considering the value of the atomic radius of pure metallic Lithium (1.52 Å) in its bcc lattice, and the one of pure metallic Lead in its fcc lattice (1.75 Å), it follows that, if both these values were kept also in the cubic cell of the β-LiPb lattice, this cell would be characterized by a cell constant of

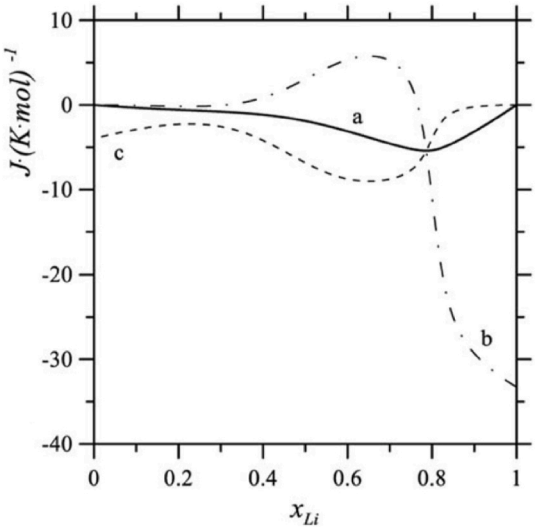

Fig. 2. a) Molar Excess mixing Entropy at 1073K as a function of Li molar fraction; b) Partial Excess Mixing Entropy of Pb; c) Partial Excess Mixing Entropy of Li [32]*
* Reprinted from Journal of Molecular Liquids, 249, S.Terlicka et al., Thermodynamic properties of Li-Pb system, 66–72, Copyright (2017), with permission from Elsevier.

~3.78 Å. Since the measured cell constant is instead 3.563 Å, it appears that the interaction between Lead and Lithium atoms in this structure is stronger than the one between atoms of the same type in pure metallic Lithium.

The Lead-Lithium bond has hence been described not as a pure metallic one, but as having a partial ionic nature, in which the electrons are not completely delocalized, but preferentially kept by the more electronegative Lead atoms. In this regard, it has been reported [11] that the ionic nature of the Lithium-Lead bond inside the many intermetallic compounds results more pronounced the higher is the Lithium content in the compound, reaching the maximum in case of Li_4Pb. A typical property which reflects the ionic behaviour of these compounds is their volumetric expansion at the melting point, which is higher than the one normally associated to pure metals: while the volumetric expansion of Lithium and Lead upon melting are, respectively, about 1.5 % and 3.56 %, for LiPb this expansion results ~9.0 % [11]. Similarly, the quit higher value of the electrical resistivity of LiPb with respect to that of both the pure metals indicates again the partial ionic nature of this intermetallic compound [11].

2.2. The Pb-Li eutectic mixture from the phase diagram

Let's focus now on the possible interaction between the two metals in the Pb-rich region of the phase diagram, i.e. when the heavier metal is more abundant, in concentration terms, than the lighter one. This condition includes also the Pb/Li atomic ratio 84.3/15.7, which corresponds to the eutectic mixture of our concern. We can discuss the system in this region forgetting the many interactions and compounds possible in the Li-rich zone, as only 2 components existed: pure Pb from one side (the right); LiPb intermetallic compound from the other (the left). Fig. 1 (right side) tells us that.

- in the top grey region, only one phase is present at equilibrium conditions: a liquid solution, where Pb and Li are fully miscible;
- in the yellow region, two phases coexist at equilibrium conditions: a solid β-LiPb phase and a liquid solution containing Pb and Li;
- in the green region, two phases coexist at equilibrium conditions: a solid Pb alloy (almost entirely Pb, with a minimum concentration of dissolved Lithium) and a liquid solution containing Pb and Li;

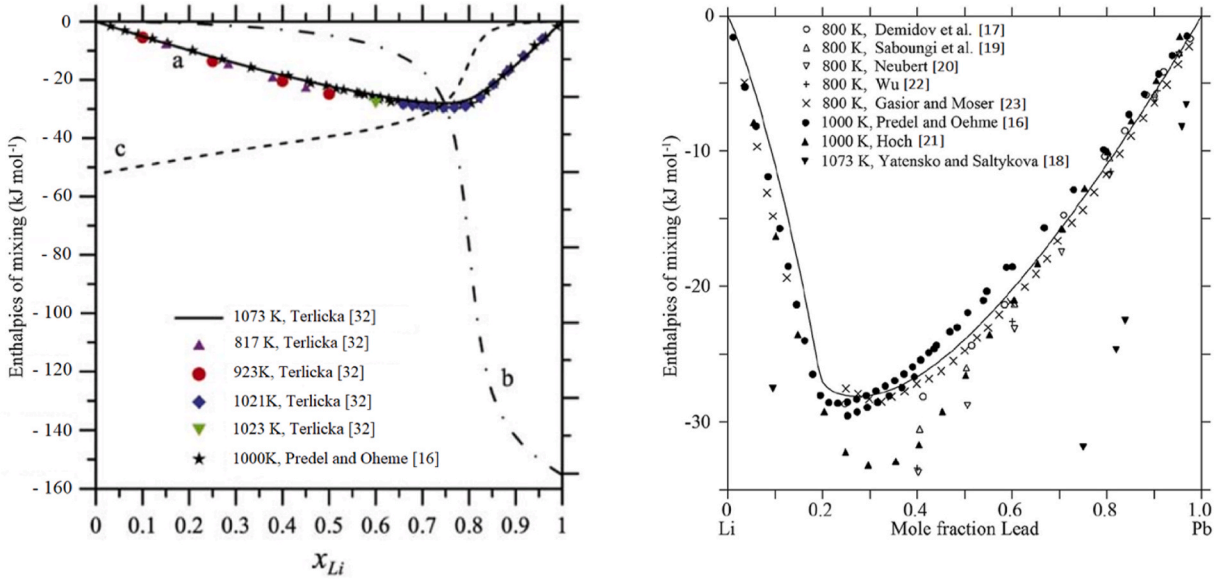

Fig. 3. Left: Molar Mixing Enthalpy (a), Partial Mixing Enthalpy of Pb (b) and Partial Mixing Enthalpy of Li (c) measured by Terlicka [32] and compared with experimental data by Ref. [16]*; right: Molar Mixing Enthalpy, calculated by Zhou [10] at 800K (continuous line), in comparison with experimental data by Ref. [16] and data calculated by other authors [17–23]**

* Reprinted from Journal of Molecular Liquids, 249, S.Terlicka et al., Thermodynamic properties of Li-Pb system, 66–72, Copyright (2017), with permission from Elsevier ** Reprinted from Journal of Nuclear Materials, 447, C.Zhou et al., Thermodynamic optimization of Li-Pb system aided by first-principles calculations, 95–101, Copyright (2016), with permission from Elsevier.

- in the eutectic point (T = 235 °C, Pb atomic fraction = 84.3 %), three phases coexist at equilibrium conditions: a solid β-LiPb phase, a solid Pb alloy (97 % of Pb + 3 % of Li, in terms of atomic fraction) and a liquid solution containing Pb and Li, which is characterized by the atomic ratio of the 2 metals exactly equal to 84.3/15.7.
- in the pink region, only one phase is present at equilibrium conditions: a solid Pb alloy (almost entirely Pb, with a minimum content of dissolved Lithium);
- in all the white regions, two solid phase coexist at equilibrium: a solid LiPb phase and the aforementioned solid Pb alloy. It must also be noted that solid LiPb would exit in its β-phase in the range of temperature between 214 and 235 °C, while below 214 °C it would be replaced by the α-LiPb phase, as evidenced by the horizontal line in the graph at 214 °C. The relative amount of the two solid phases (Pb and LiPb) that coexist in the white regions of Fig. 2 can be evaluated, as for all the phase diagrams, through the lever rule.

If we consider to apply the level rule to the exact eutectic composition, we get for the 2 solid phases in equilibrium the following relative abundances, in molar terms:

phase 1 = β-LiPb phase: ~0.27

phase 2 = solid Pb alloy (97% of Pb + 3% of Li): ~0.73

This means that, when a liquid alloy characterized by the eutectic composition (which is the alloy of our concern) is cooled down to solidification, 2 different solid phases form, with the relative abundance above reported. These 2 phases arrange in narrow, separate, layers, which alternate one above the other, giving rise to a very fine lamellar structure.

It must be anyway observed that some authors, especially before the experimental work made by Hubberstey in 1992 [2], proposed a slightly different phase diagram, which located the β-LiPb/Pb eutectic in correspondence of a Lead concentration equal to 83 %, i.e. a bit smaller of the value now assumed as correct. Consequently, values reported in their papers for the thermophysical properties of the eutectic Pb-Li actually resulted from experimentations conducted on samples characterized by such a smaller Pb/Li atomic ratio. This fact, as will be seen in section 4, introduces a kind of inhomogeneity in the ensemble of all the compared experimental data, anyway it must be underlined that, in many cases, the differences in the values of these data are so high (even orders of magnitude) to make trivial the possible effect arising from a difference in composition of only 1.7 %.

2.3. The Pb-Li liquid solutions

The nature of the liquid Li-Pb solution can be described through the analysis of the values assumed by its excess thermodynamic functions, i. e. the difference between, respectively, the mixing Gibbs Free energy, the mixing Enthalpy and the mixing Entropy of the real solution, and the corresponding mixing functions of an ideal solution at the same composition, temperature and pressure, as indicated by the general equation (1):

$$Z^E = \Delta_{mix}Z - \Delta^{ideal}{}_{mix}Z \quad (1)$$

where Z^E is a generic excess thermodynamic function and $\Delta_{mix}Z$ and $\Delta^{ideal}_{mix}Z$ are, respectively, the real mixing value and the ideal mixing value associated to the function Z.

While for an ideal solution the mixing Enthalpy ($\Delta^{ideal}_{mix}H$) is always 0, this is not true for the mixing Entropy ($\Delta^{ideal}_{mix}S$), because the presence of more than one chemical species in the solution (in our cases 2 components: Li and Pb) originates several ways of reciprocally dispose the different atoms inside the phase. In mathematical terms, the ideal mixing Entropy for a solution constituted by only 2 components (A and B), is given by:

$$(\Delta^{ideal}{}_{mix}S) = -R\,[n_A \ln(x_A) + n_B \ln(x_B)] \quad (2)$$

where R is the ideal gas constant, and n_A and x_A are, respectively, the number of mols and the molar fraction of the A component in the solution.

Rarely a solution behaves as an ideal one: the more it deviates from the ideal behaviour, the higher its excess thermodynamic quantities will differ from 0. The deviation from ideality becomes the rule when the electronegative difference between the constituents is large as in Li-Pb

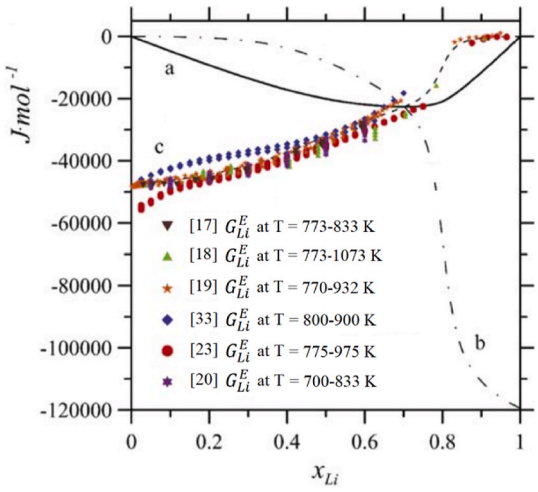

Fig. 4. Molar Excess mixing Gibbs free energy as a function of Li molar fraction (a), Partial Excess mixing Gibbs free energy of Pb (b) and Partial Excess mixing Gibbs free energy of Li (G_{Li}^E) (c) at 1073K [32], also compared with previous evaluations*

* Reprinted from Journal of Molecular Liquids, 249, S.Terlicka et al., Thermodynamic properties of Li-Pb system, 66–72, Copyright (2017), with permission from Elsevier [33].

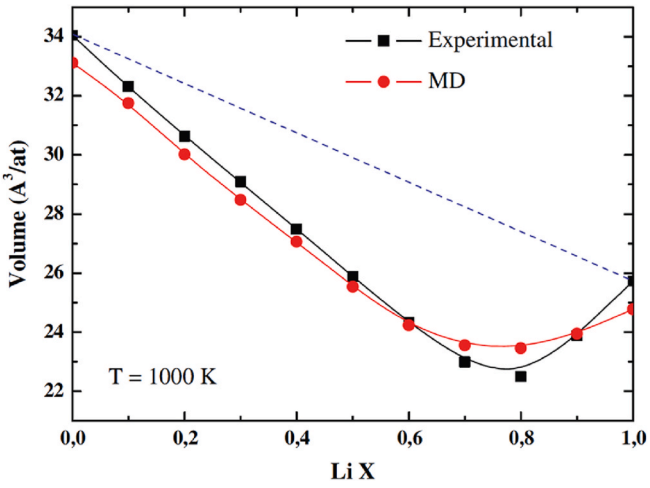

Fig. 5. Liquid alloy volume as a function of the composition at 1000K. Blue dashed line: ideal behaviour; black curve: experimental values achieved by Saar [34]; red curve: output of the MD simulation [27]*

* Reprinted from Journal of Nuclear Materials, 448, A.Fraile et al., Interatomic potential for the compound-forming Li-Pb liquid alloy, 103–108, Copyright (2014), with permission from Elsevier.

case (1.35 in Pauling scale). Here, electron transfer from Li to Pb gives rise, at specific compositions, to ionic bonding and preferred heterocoordination: Li-Pb systems belong to the class of alloys having a salt-like arrangement and no covalent bonding [15].

The proper evaluation of the excess quantities permits to infer, through different theoretical models, important solution parameters, like the average interatomic distances and the activity coefficients; moreover, the variation of the excess quantities with the solution composition can also indicate the existence of some particular interaction or organization inside the solution, associated to a specific formal stoichiometry. In this regard, basing also on the results of previous experimental activities [16–25], Mudry [26] studied $Pb_{83}Li_{17}$ liquid alloys (close to the eutectic composition) through the X-ray diffraction method and used the experimental structure data to calculate the partial structure characteristics by means of Reverse Monte Carlo method; Fraile [27] modelled the Li-Pb system at the atomic scale employing Molecular Dynamics simulation based on the Embedded Atom Method (EAM) potentials; Zhou [10] adopted an associate solution model and made its calculation with the VASP [28–31] software based on DFT-GGA (Density Functional Theory – Generalized Gradient Approximation); Terlicka [32] measured the mixing enthalpy of liquid Li-Pb alloys and proposed the new *Qualitative Associates Model* to determine the excess Gibbs energy variations with temperature and composition.

The modelizations made by all these authors lead to descriptions of the Pb-Li system which are generally congruent and, in many cases, are able to closely reproduce the experimental results. Without entering into the complex details of their calculations, we report below, with the help of some pictures, the outcome of some of them, in terms of the above-mentioned thermodynamic functions, together with some general conclusions.

Fig. 2 shows the Molar Excess mixing Entropy (S^E), together with the Partial Excess Entropy of Pb and of Li (partial quantities give the contribution of only one of the two components of the solution: the total Molar Excess quantity is given by the sum of the partial ones, each one multiplied by the corresponding molar fraction), as evaluated by Terlicka [32] at 1073K. S^E is clearly 0 when $x_{Li} = 0$ or 1 (in these cases there is actually only 1 component in the solution), while for all the other compositions it assumes negative value, indicating that $\Delta_{mix}S$ is always $< \Delta_{mix}^{ideal}S$ and that a kind of organization (order) has been established in the liquid solution; the maximum (in absolute value) is in correspondence of X_{Li}~0.8.

Similarly, Fig. 3, on the left, shows the Molar Mixing Enthalpy ($H^E = \Delta_{mix}H$), together with the Partial Mixing Enthalpy of Pb and of Li, obtained by Terlicka [32] at various temperatures; the same quantity (H^E), calculated by Zhou [10] and compared with many experimental results, is shown instead on the right. Also this thermodynamic function assumes negative values all over the composition range, with small changes with the temperature (Fig. 3 left) and a good agreement with the experimental data measured by Predel [16]; a minimum value is present in correspondence of $x_{Li} \sim 0.75–0.8$. The trend of H^E is the same on both the left and the right side of Fig. 3: on the right, anyway, some data evaluated from previous references [18,20,21] appear a bit distant from those calculated by Ref. [10].

Fig. 4 shows the values calculated by Ref. [32] for the Molar Excess mixing Gibbs free energy (G^E) at 1073K, as a function of the solution composition, together with the Partial Excess mixing Gibbs energy of Lead and Lithium (G_{Li}^E); the good agreement with most data coming from previous experimentations for the latter quantity is evident. Here again the values are always negative, with a minimum value assumed by G^E for x_{Li} ~0.75–0.8. The trend of G^E is actually similar to the one of H^E in Fig. 3, since S^E adds only a smaller contribution in absolute value (Fig. 2), and G^E is clearly a bit less negative than H^E. By looking on the whole at Figs. 2–4, it is possible to verify that the interactions between heteroatoms in solutions reach their maximum for a Li concentration around 0.75–0.8 at.%, and this makes sense since, if we look also at the phase diagram of the Pb-Li system in Fig. 1, we see that this range of compositions corresponds to those solid compounds, like Li_4Pb, $Li_{10}Pb3$, Li_3Pb, which are characterized by the highest melting point; the formation of clusters or associates with similar stoichiometries is hence expected to takes place in solution as well [23].

Another interesting picture of the system is given by the analysis of the liquid alloy volume versus the composition, as shown in Fig. 5 [27]. Here, the atomic volume is always smaller than the ideal case (weighted average of the pure liquid metals) and exhibits a minimum value (maximum contraction) for $x_{Li} \sim 0.8$, suggesting the possible Li_4Pb compound formation in solution. Consequently, the density of the solution will result higher than in the ideal case (this aspect will be examined in depth in section 4.2).

It must be observed that the formation of Pb-Li associates, particularly those corresponding to the formal stoichiometry Li_4Pb, was evidenced by some authors [26,27] also according to the Structure Factors

and the Partial Structure Factor (PSF) calculated starting from X-ray and neutron scattering analysis of the solution.

Additionally, Terlicka [32] proposed the existence also of Pb-Li associates (i.e. with 1:1 atomic ratio), basing on the evaluation of the Warren-Cowley Short Range Order (SRO) parameter [35–38]. The value of this parameter may in general vary in the range $-1 \div 1$: when negative, it indicates that in the liquid solution the interaction between different atoms is much stronger than between the same atoms and that hetero-atoms associates may form; conversely, if SRO is positive, the interaction between atoms of the same kind is stronger and hetero-association is impossible, with the consequent tendency to segregation. Terlicka [32] showed that the Pb-Li solutions assume SRO values ≤ 0 all over the composition range, with a minimum (SRO ~ -0.75) in correspondence of $x_{Li} = 0.8$ (ascribed to the abovementioned Li_4Pb associate), but also an inflexion point in correspondence of $x_{Li} = 0.5$, which would suggest the existence of Li-Pb associates as well; therefore, the degree of association in solution changes with the specific solution composition.

Of course the description of the Pb-Li solution at the eutectic composition ($x_{Li} = 15.7$ at.%), particularly around 300 °C, is the most interesting aspect for the purpose of fusion applications. Some investigation was conducted specifically by Mudry [26], even if he assumed for the eutectic composition the old accepted value of $x_{Li} = 17$ at.%. Through the X-ray diffraction technique and the following analysis of the Partial Structure Factors, he evaluated that the distance between the first Pb-Pb neighbours in $Pb_{83}Li_{17}$ melt at 508K is larger (3.55 Å) than in pure liquid Pb (3.33 Å), while the Pb-Li distance (2.79 Å) is significantly less than in the assumption of a random atomic distribution (3.3 Å). From all these values, the author inferred the existence of Li_4Pb atomic associates (ordered structural units also called Zintl ions) randomly distributed in a Pb-matrix (Pb_n clusters), therefore he defined rather inhomogeneous the Pb-Li melt. Additionally, while increasing the temperature from 508K to 593K didn't affect substantially the Pb-Pb (3.55 → 3.54 A) and the Pb-Li (2.79 → 2.77A) distances, it augmented instead the Li-Li one (2.40 → 2.76 A), indicating that the Pb-matrix kept its structure, while some Li atoms detached from the associates and diluted inside the Pb-matrix.

3. Methods

In the next sections we will look in details at the thermophysical properties of the Pb-Li eutectic liquid solution which are considered the most important for the design and simulation of the WCLL blanket concept, namely.

- Specific Heat;
- Density;
- Volumetric thermal expansion;
- Thermal conductivity;
- Thermal diffusivity;
- Electrical resistivity;
- Sievert's constant.

After retrieving, for each of the above properties, the many values and correlations reported in literature, they have been compared, searching for the most trustable of them, in order to finally reach (hopefully) a clear description of the Pb-Li system. To assess the soundness of each specific correlation, the following aspects have been generally evaluated.

- the validity of the employed experimental setup and working procedure;
  (this includes the conceptual nature of the experiment, the purity of the employed materials, the bigger or smaller number of independent measurements, the drawbacks reported by the author himself ….)
- the intrinsic results goodness;
  (which is the reproducibility of the results? is the reported correlation able to fit properly the experimental data? which is the effect of changing one of the test conditions on the experiment outcome?)
- the closeness of the experimental conditions to the Pb-Li working conditions in the blanket;
  (the closer they are, the smaller will result the error lying in the interpolation/extrapolation of the experimental data)
- the distance of the set of values collected in a specific experiment from the average of the whole data ensemble and the explanation given by the author to justify why his results differ from the others'.

Finally, since the abovementioned properties, according to their definitions, are in many cases directly linked, it is also important that the ensemble of all the equations selected for their descriptions is characterized by a good internal coherence, i.e. it doesn't lead to contradictory results in the calculated values.

The outcome of this analytical work is reported in the following Results section, with a dedicated subsection for each of the thermophysical property. Each subsection entails a short theoretical premise (to introduce the topic and the equations later employed), presents the collection of the available experimental data and finally analyze them to find out the best correlation.

4. Results

4.1. Specific heat (c_p)

4.1.1. Theoretical premise

Specific heat (c) of a substance is defined as its thermal capacity (C) divided by its mass; it corresponds therefore to the heat required to raise the temperature of one gram of substance by one Kelvin degree. In case we consider a system at constant pressure (usual case of interest), the corresponding thermal capacity, C_p, becomes:

$$C_p = \frac{\partial H}{\partial T} \tag{3}$$

and the specific heat, c_p, becomes hence:

$$c_p = \frac{\partial H}{\partial T}\ \frac{1}{m} \tag{4}$$

where H [J] is the enthalpy, T [K] is the temperature and m [g] is the mass of the substance; the unit of measurement of c_p is hence [J g^{-1} K^{-1}]. It must be observed that, in the above equations, the value of H is considered positive when heat is entering the system: since such an energy transfer always determines a positive increase of the temperature, it follows that c_p always assumes positive values as well. Of course it is possible to define also a thermal capacity per mol of substance instead of mass of substance: in this case the *molar thermal capacity,* C_{pm} [J mol^{-1} K^{-1}], can be simply obtained from c_p by multiplying it for the molar mass of the substance, M [g mol^{-1}].

Considering that the value of H of each substance increases with the amount of substance (H is an extensive thermodynamic quantity), it follows that, in case of a system containing more than a single component, as is the case of our eutectic solution, H can be calculated by adding the enthalpy of each component. Anyway, as we have seen in section 2.3 (Fig. 3), the enthalpy of each component in a solution or mixture is different from that of the component when alone; the enthalpy of mixing ($H^E = \Delta_{mix}H$), which is 0 only for ideal systems, must be summed as well in the evaluation of the total enthalpy of real systems, introducing consequently an additional contribution in the evaluation of the thermal capacity (and of the specific heat).

So, if the total enthalpy of the eutectic Pb-Li solution is given by:

$$H(eut) = H(Pb) + H(Li) + \Delta_{mix}H \tag{5}$$

Table 2
Experimental c_p vs T correlations available in literature for the Pb-Li for 'near eutectic' solutions.

Author	Li content [mol %]	Method	Correlation	Range of T [K]	Ref.
Reiter	17.0	Calvet Differential Calorimeter	c_p [J g^{-1} K^{-1}] = 0.2259 + 1.347 · 10^{-3} T [K] – 2.557 · 10^{-6} T^2 [K^2]	508–573	[39]
Kuhlborsch	17.0	Calvet Differential Calorimeter	c_p [J g^{-1} K^{-1}] = 0.6271–7.908 · 10^{-4} T [K]	508–573	[40]
Schulz	16.8	Differential Scanning Calorimeter	c_p [J g^{-1} K^{-1}] = 0.195–9.116 · 10^{-6} T [K]	508–800	[43]

where H(y) it the enthalpy of the element (y), the corresponding thermal capacity results:

$$C_p(eut) = \frac{\partial H(Pb)}{\partial T} + \frac{\partial H(Li)}{\partial T} + \frac{\partial mixH}{\partial T} = C_p(Pb) + C_p(Li) + \Delta C_p \quad (6)$$

where C_p(y) is the thermal capacity of the element (y), while

$$\Delta C_p = \frac{\partial mixH}{\partial T} \quad (7)$$

is the additional contribution to thermal capacity coming from the not ideal behaviour of the solution.

Considering that C_p of each element corresponds to its C_{pm} multiplied by the quantity of substance [mol], it is also possible to write:

$$C_{pm}(eut) = C_{pm}(Pb) \cdot x_{Pb} + C_{pm}(Li) \cdot x_{Li} + \Delta C_{pm} \quad (8)$$

Equation (8) hence permits (as detailed later, in section 4.1.3) to make a theoretical prevision of the expected values of C_{pm} (hence of c_p) of the eutectic solution on the basis of the values, available in literature, of C_{pm} of pure Pb, pure Li and ΔC_{pm}. In any case, we expect that the value of C_{pm}(eut) will be not very different from the values of C_{pm} of both pure Pb and pure Li. C_{pm}(Pb) and C_{pm}(Li) in fact assume very similar values (this similarity is typical of almost all metals), therefore each combination of them, normalized on the basis of the molar fractions, cannot be too different as well; additionally, the contribution given by the non ideality of the system (ΔC_{pm}) is rather small with respect to the pure components contribution.

4.1.2. *Experimental c_p data from literature*

The ensemble of c_p data achieved through a direct calorimetric measurement of Pb-Li eutectic liquid solution is indeed rather small [39,40,43] (Table 2); additionally, an indirect determination of c_p was obtained through the measurement of the solution density and of its adiabatic temperature variation with pressure [34]; later, other theoretical works were presented [41,42], proposing anyway only a rearrangements of the previous data based on different calculation strategies.

Reiter [39] and Kuhlborsch [40] employed a Calvet differential calorimeter to get the values of c_p up to 300 °C, anyway their results appear very strange, because in both cases c_p assumes a too high value at the eutectic melting point and decreases too much with temperature: keeping that trend, it would reach the value of 0 in few hundreds of degree.

Later Schulz [43], which also evidenced the anomaly of the aforementioned evaluations, performed a new calorimetric experiment, investigating an alloy characterized by a Li content equal to ~ 0.67 wt% (which corresponds to about 16.8 at.%), i.e. a bit richer in Li with respect to the value currently defined for the eutectic composition (15.7 at.%). He prepared the alloy starting from Li (99.4 % purity) and Pb (99.9 % purity) and operating under Argon atmosphere; for the measurement he employed a *PerkinElmer* differential scanning calorimetry, calibrated against a sapphire. Its results, investigating the temperature range 508–800K, are graphically shown in Fig. 6.

From the interpolation of the data, got from 2 different samples, he proposed the following linear correlation:

$$c_p \text{ [J g}^{-1} \text{ K}^{-1}\text{]} = 0.195\text{–}9.116 \cdot 10^{-6} \text{ T} \quad (9)$$

where T is expressed as absolute temperature [K].

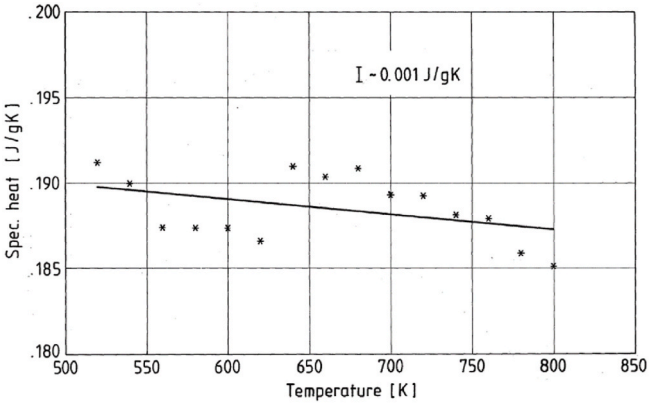

Fig. 6. Experimental c_p values achieved by Schulz [43], together with the linear fitting equation*
* Reprinted from Fusion Engineering and Design, 14, B.Schulz, Thermophysical properties of the Li(17)Pb(83) alloy, 199–205, Copyright (1991), with permission from Elsevier.

Additionally, Schulz also compared his results with the ones already reported by Saar [34] at 1000K, which weren't anyway achieved through a direct calorimetric method but by means of measurements of the solution density and of its adiabatic temperature variation with pressure: after extrapolating his own results at 1000K, he found a good data agreement with them. A more recent theoretical analysis of the available c_p data [44] also confirmed the soundness of equation (9).

4.1.3. *Indirect evaluation of the c_p data: optimization of the correlation*

Equation (9), even if considered the most trustable experimental correlation for the c_p values, is anyway related to a composition not exactly matching the real eutectic one (x_{Li} = 0.168 instead of 0.157). Additionally, the trend of the c_p values with temperature seems too flat, if compared with the c_p trends of both pure Li and pure Pb, which on the average decrease more. Actually, if we look at Fig. 6, we see a strange positive jump in c_p values (even if small in absolute terms) going from ~620 to ~ 640K: it would seem as all the values at 640K and beyond were shifted by a positive terms with respect to the ones at lower temperatures. In this regard, it could be possible to think that the c_p values at lower temperatures were obtained from the investigation of a specific Pb-Li sample, while those at higher temperatures would be obtained instead from a different Pb-Li sample, slightly richer in Lithium (c_p of pure Li is in fact bigger than pure Pb one, therefore, the more is the Li content, the higher is the solution c_p). This hypothesis seems supported by the fact that, considering separately the 2 sets of data, visually their trends with temperature result indeed rather similar, and more negative (as expected) than the one described by equation (9).

Basing on this observation, we search hence to get a better mathematical description of the experimental data and to reach a slightly improved correlation, adapted to the real eutectic composition. To do so, we employ the already discussed equation (8) for the Molar Thermal capacity (C_{pm}) of the solution.

$$C_{pm}(eut) = C_{pm}(Pb) \cdot x_{Pb} + C_{pm}(Li) \cdot x_{Li} + \Delta C_{pm} \quad (8)$$

and we consider the rather reliable values tabulated in literature for

Table 3
Values of C_{pm} and c_p for the Pb-Li solutions calculated starting from pure components data.

T [K]	C_{pm}(Li) (x_{Li} = 1) [j mol^{-1} K^{-1}]	C_{pm}(Pb) (x_{Li} = 0) [j mol^{-1} K^{-1}]	Ideal C_{pm} (x_{Li} = 0.168) [j mol^{-1} K^{-1}]	Real C_{pm} (x_{Li} = 0.168) [j mol^{-1} K^{-1}]	c_p (x_{Li} = 0.168) [J g^{-1} K^{-1}]	Ideal C_{pm} (x_{Li} = 0.157) [j mol^{-1} K^{-1}]	Real C_{pm}(x_{Li} = 0.157) [j mol^{-1} K^{-1}]	c_p (x_{Li} = 0.157) [J g^{-1} K^{-1}]
			note:ΔC_{pm} = 0	note: ΔC_{pm} = 2.35	note: M = 173.55	note: ΔC_{pm} = 0	note: ΔC_{pm} = 2.35	note: M = 175.76
500	30.125	30.945	30.807	33.157	0.19105	30.816	33.186	0.18870
600	29.539	30.635	30.451	32.801	0.18899	30.463	32.813	0.18669
700	28.987	30.332	30.106	32.456	0.18701	30.121	32.471	0.18475
800	28.937	30.016	29.835	32.185	0.18544	29.847	32.197	0.18319
900	28.886	29.698	29.562	31.912	0.18387	29.571	31.921	0.18162
1000	28.836	29.397	29.303	31.653	0.18238	29.309	31.659	0.18013

C_{pm}(Li) [45] and C_{pm}(Pb) [46][2] while, for ΔC_{pm}, those reported by Refs. [27,32,34,47] and affected by a bit larger uncertainty. C_{pm}(Li) and C_{pm}(Pb) values at different temperatures are reported in Table 3, respectively in the 2nd and the 3rd column.

Starting from C_{pm}(Li) and C_{pm}(Pb) it is possible, applying equation (8), to calculate at each temperature the correct value of C_{pm} of a Pb-Li solution characterized by a Li at.% = 16.8, i.e. the same composition of the sample investigated by Schulz, in the assumption of an ideal system, i.e. if $\Delta_{mix}H$ and consequently ΔC_{pm} were equal to 0. The corresponding quantity is indicated as **Ideal C_{pm} (x_{Li} = 0.168)** in the 4th column of Table 3. The Molar Thermal Capacities of the real solutions, **Real C_{pm} (x_{Li} = 0.168)** in the 5th column of Table 3, have been then obtained at each temperature by adding to the ideal ones the constant ΔC_{pm} = 2.35 J mol^{-1} K^{-1}; finally, the specific heat of the Pb-Li solutions resembling the Schulz samples have been obtained by dividing the previous values by the Molar Mass of this solution (173.55 g mol^{-1}), and reported as **c_p(x_{Li} = 0.168)** in the 6th column of Table 3.

Regarding the choice of the specific value of 2.35 J mol^{-1} K^{-1} for ΔC_{pm}, it must be said that this value is the one that allows the calculated specific heats of the solutions to best reproduce the experimental values of Schulz graphically reproduced in Fig. 6 (the comparison is only visual, since Schulz didn't report its experimental data in numerical form). Additionally, it must be said that this value is in good agreement with [32,42,47], which calculated for ΔC_{pm} a value in the range of 1.5–3 J mol^{-1} K^{-1} in the surrounding of the eutectic composition, also indicating its substantial constancy with temperature.

In order to calculate now the specific heat of the Pb-Li solution characterized by x_{Li} = 0.157, we can follow exactly the same procedure as before, keeping for this slightly different composition the same value of ΔC_{pm}, since, according to Refs. [32,34,47], its value is expected to change trivially for small composition shift in Pb-rich solutions (the value of ΔC_{pm} increases instead significantly for Li-richer solutions; particularly for x_{Li} = 0.5 it was calculated as 5.2 ± 1.4 J mol^{-1} K^{-1}, while for x_{Li} = 0.78 it increased up to 15.7 ± 2.4 J mol^{-1} K^{-1} [47]). The ideal and the real molar thermal capacities of the x_{Li} = 0.157 solution are reported as **Ideal C_{pm} (x_{Li} = 0.157)** and **Real C_{pm} (x_{Li} = 0.157)** respectively in the 7th an 8th columns of Table 3; finally, the specific heats of this solution **c_p(x_{Li} = 0.157)** are calculated after dividing the real thermal capacities for the solution Molar Mass, which assumes now the value of 175.76 g mol^{-1} (9th column). From the values reported in Tables 3 and it's easy to note that the differences between the values of the specific heats of the solutions at different compositions arise mainly from their different Molar Masses; in fact, as already stated, the molar thermal capacity is minimally affected by the compositions variation (compare the values in 5th and 8th columns).

The values of the specific heats of the 'real' eutectic solution at different temperatures are graphically displayed in Fig. 7, together with the best fitting line. The selected fitting equation is actually a 'functional' equation, since, considering the theoretical complexity of the system, it is not possible to fix a specific type of dependence on T. A second order polynomial equation has been hence selected, which is able to give a better description of the data trend (R^2 = 0.9997) respect with a first order (linear) one. It is below reported:

$$c_p\ [J\ g^{-1}\ K^{-1}] = 0.2009 – 2.806 \cdot 10^{-5}\ T + 7.343 \cdot 10^{-9}\ T^2 \quad (10)$$

The second order term introduces only a very small correction in the final result, while the first order term is indeed almost the triple of the Schulz one in equation (9), since it reflects mainly the trend with temperature of the specific heat of pure liquid Lead.

To conclude, it can be said that the procedure here employed to

[2] It must be noted that the values of C_{pm}(Pb) at temperatures below Pb melting point were evaluated in Ref. [46] as if this metal was still in liquid phase, therefore they cannot be experimental values, but they are obtained by extrapolating down the liquid phase molar thermal capacity of Pb.

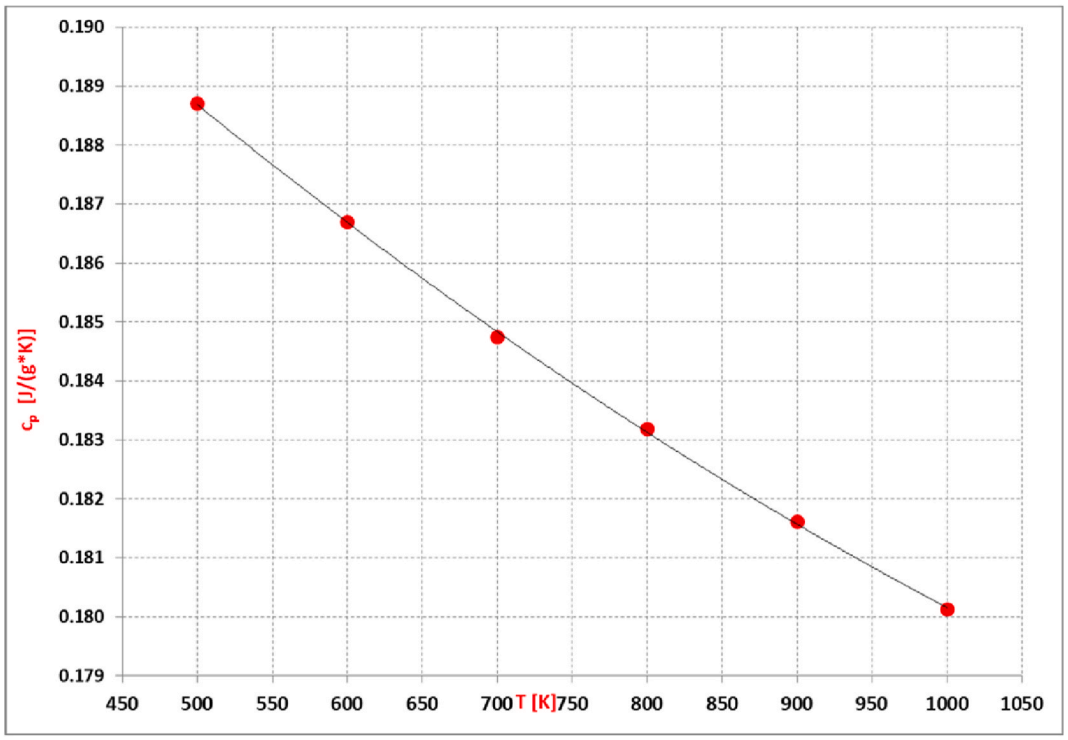

Fig. 7. Calculated c_p for the eutectic Pb-Li solution (Li = 15.7 at.%), together with their fitting line.

Table 4
Experimental ρ vs T correlations available in literature for the Pb-Li 'near eutectic' solutions.

Author	Li content [mol %]	Method	Correlation	Range of T [K]	Ref.
Schulz	16.8	Sessil drop	ρ [Kg m^{-3}] = 10450–1.68 T [K]	508–625	[43]
Alchagirov	17.0	Pycnometric	ρ [Kg m^{-3}] = 9912–0.798 T [K]	580–770	[54]
Prokhorenko	17.0	Penetrating γ-rays	ρ [Kg m^{-3}] = 10470–1.152 T [K]	508–900	[56,57]
Stankus	17.0	Penetrating γ-rays	ρ [Kg m^{-3}] = (10520.35 ± 3.96) – (1.19501 ± 0.00558) T [K]	508–880	[58]
Khairulin	15.7	Penetrating γ-rays	ρ [Kg m^{-3}] = (10581.8 ± 35.5) – (1.229 ± 0.027) T [K]	508–997	[59]

calculate c_p of the Pb-Li eutectic liquid solution, can be applied as well to any Pb-Li solution characterized by a slightly different composition (Δx_{Li} of the order of ±1 at.% or a bit more), for which ΔC_{pm} can be assumed to be equal to that of the eutectic one. Since x_{Pb} corresponds to $(1\text{-}x_{Li})$, it is possible to rewrite equation (8) for a generic 'close to eutectic' solution as:

$$C_{pm}(sol) = C_{pm}(Pb)\cdot(1\text{-}x_{Li}) + C_{pm}(Li)\cdot x_{Li} + \Delta C_{pm}(sol) = C_{pm}(Pb) + x_{Li}\cdot [C_{pm}(Li) - C_{pm}(Pb)] + \Delta C_{pm}(sol) \quad (11)$$

Dividing by the molar mass of the solution (which also depends on the composition and the molar masses of Lithium and Lead, respectively M_{Li} and M_{Pb}) we get the generic relation for the corresponding specific heat:

$$c_p(sol)\ \left[J\ g^{-1}\ K^{-1}\right] = \frac{C_{pm}(Pb) + x_{Li}\ [C_{pm}(Li) - C_{pm}(Pb)] + C_{pm}(sol)}{M_{Pb} + x_{Li}\ (M_{Li} - M_{Pb})} = \frac{C_{pm}(Pb) + x_{Li}\ [C_{pm}(Li) - C_{pm}(Pb)] + 2.35}{207.2 - 200.3\ x_{Li}} \quad (12)$$

4.2. Density and volumetric thermal expansion coefficient

4.2.1. Theoretical premise

Density (ρ) and volumetric thermal expansion coefficient (β) are two linked properties of the solution, in that both of them follows from the same quantity, the molar volume, and its variation with temperature: therefore, they will be together dealt with in this section.

If we consider exactly 1 mol of material, density is in fact given by the relation:

$$\rho = \frac{M}{V_m} \quad (13)$$

where M is the molar mass and V_m is the molar volume. The volumetric thermal expansion coefficient, by definition, is instead given by:

$$\beta = \frac{1}{V_m}\ \frac{\partial V_m}{\partial T} \quad (14)$$

which, introducing V_m as (M/ρ) according to equation (13), becomes:

$$\beta = \frac{\rho}{M}\ \frac{\partial\left(\frac{M}{\rho}\right)}{\partial T} = \rho\left(-\frac{1}{\rho^2}\right)\ \frac{\partial}{\partial T} = -\frac{1}{\rho}\ \frac{\partial}{\partial T} \quad (15)$$

Therefore, in this section, the most trustable correlation for the density will be at first searched for, by analysing the many experimental data reported in literature. Then, the volumetric expansion coefficient will be got by simply applying equation (15) to the selected expression for density: this way, the internal coherence of the two quantities will be assured.

Of course, if the Pb-Li eutectic solution behaved as an ideal solution, its molar volume could be simply calculated from the available knowledge of the molar volumes of the 2 pure metals, since volume is an

extensive quantity; unfortunately, the non ideality of the system introduces the additional V_m^E term, i.e., the molar excess mixing volume, so that a relation formally equal to equation (11) actually holds for the molar volume of the solution:

$$V_m(sol) = V_m(Pb) + x_{Li} \cdot [V_m(Li) - V_m(Pb)] + V_m^E \quad (16)$$

and a relation analogous to equation (12) actually holds for the density (ρ) of the solution:

$$\rho = \frac{207.2 - 200.3\ x_{Li}}{V_m(Pb) + x_{Li}\ [V_m(Li) - V_m(Pb)] + V_m^E} \quad (17)$$

Anyway, it is not easy to a priori estimate the V_m^E value; we only know that for the Pb-Li solutions it assumes negative values (see Fig. 5), in other words there is a volume contraction in a real Pb-Li system respect with an ideal one, and density is hence higher than for an ideal case. This effect, indicated by all the experimental investigations (see next section), actually agrees with the knowledge of the system (section 2.3), which is characterized by a strong interaction between hetero atoms and by a Pb-Li distance smaller than in the assumption of a random atomic distribution.

4.2.2. Experimental density data from literature

Several sets of values have been reported in literature for the densities of liquid Pb-Li solutions and even more correlations to describe their variations with temperature [48]: they are listed in Table 4. It must be observed, anyway, that the difference, at each temperature value, between the highest and the lowest proposed density value is always ≤3.5 % (with respect to the highest one): this likeness of values, which follows from the relative ease in the measurement of densities and from the extensive nature of the volume, assures that in any case we would not introduce important inaccuracies in the choice of a specific correlation instead of another one. Let's try however to find out the most trustable one.

The first experiment aimed at measuring the density of a Pb-Li liquid solution was reported by Schneider in 1954 [49], but it was related to a solution characterized by a Lithium molar fraction equal to 37.74 %, in the range of temperature of 500–700 °C. Later, in 1976, Ruppersberg and Speicher [50] performed many measurements of different Pb-Li solutions, covering the entire range of composition, from pure Lithium to pure Lead, but not in correspondence of the exact eutectic composition (their closest measurement was for $x_{Li} = 0.2$). In both the aforementioned investigations [49,50], the employed technique was the Maximum Pressure Gas Bubble (MPGB), which is based on the measurement of the pressure in the bubbles blown into the liquid through a capillary of known radius: the density of the liquid is estimated from the pressure change with the immersion depth of the capillary [51,52].

Density values achieved by Ref. [50], even if considered rather trustable and therefore reported in many following works [34] and collections of Pb-Li properties, suffer anyway the limit of not giving a direct picture of the real eutectic composition, which is possible only through the interpolation of the experimental data; in this regards, several, different procedures for the interpolation of those data were later proposed [40,42], but it isn't actually easy to evaluate the accuracy of these analytical processes.

A different experimental investigation was conducted (1986) by Schulz [43] on the same Pb-Li sample already described in the Specific Heat section of this document (4.1), i.e. characterized by a Li content equal to ~0.67 wt% (about 16.8 at.%) and prepared under Argon atmosphere starting from 99.4 % purity Li and 99.9 % purity Pb. For the acquisition of the density values with temperature he employed the uncommon 'sessile drop' method, using an apparatus which had been previously employed for another purpose, i.e. the contact angle measurements [53]: here, the density could be calculated from the measurements of the volume and the weight of the deposited droplet. Nonetheless, some uncertainties are present in the results so achieved,

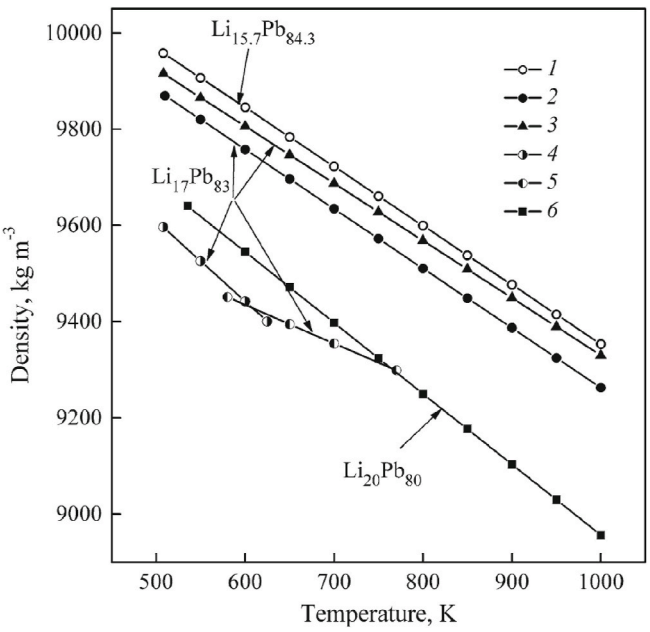

Fig. 8. Temperature dependencies of the density of liquid Pb-Li alloys of near-eutectic composition: 1 [59]; 2 [59]; 3 [58]; 4 [43]; 5 [54]; 6 [34]*
* Reproduced from International Journal of Thermophysics, R.A.Khairulin et al., Volumetric Properties of Lithium–Lead Melts, (2017) 38:23, Springer, with permission from SNCSC.

arising from the effect of gravity which deforms the shape of the droplet from a perfect sphere (and makes harder to exactly estimate its volume), from the precision in the temperature acquisition and mostly from the depth in the focus of the optical system: on the whole, the relative std. deviation of the measurement was estimated by the author as ± 3 %.

In 2005 Alchagirov [54] performed 2 series of density measurements with increasing temperature of a Pb-Li solution characterized by $x_{Li} = 0.17$, employing the pycnometric method, and calculated the confidence error of the results as ≤ 0.2 %. Its results agree with those achieved by Schulz [43], within the confidence error of the latter.

Another current of liquid materials density measurements is instead based on the penetrating γ-rays technique, which entails to monitor the attenuation of the intensity of a flux of γ-radiation passing through the material. Density can be calculated, at a specific temperature (T), through the formula:

$$\rho(T) = \frac{\ln [J_0(T)/\ J(T)]}{d(T)} \quad (18)$$

where J(T) and $J_0(T)$ are, respectively, the intensity of the radiation after its passage through the crucible containing or not the sample, d(T) is the γ-rays attenuation length (the inner diameter of the crucible corrected for the γ-rays beam diameter; d is function of temperature, because solid crucible changes a bit its geometry with temperature) and μ is the mass attenuation coefficient of the investigated material (this quantity instead doesn't depend on temperature, nor on the aggregation state of the materials, but only on the nature of the nucleus of the material and of the specifically employed γ-rays beam). For what concerns a multicomponent system, as our eutectic Pb-Li solution, the mass attenuation coefficient (μ_{sol}) can be calculated using the additivity rule, according to the formula [55]:

$$\mu_{sol} = \sum \mu_i c_i \quad (19)$$

where μ_i and c_i are respectively the mass attenuation coefficient and the mass concentration of each component of the system. In the case of the Pb-Li eutectic solution, whose values of c_i are known since fixed by the

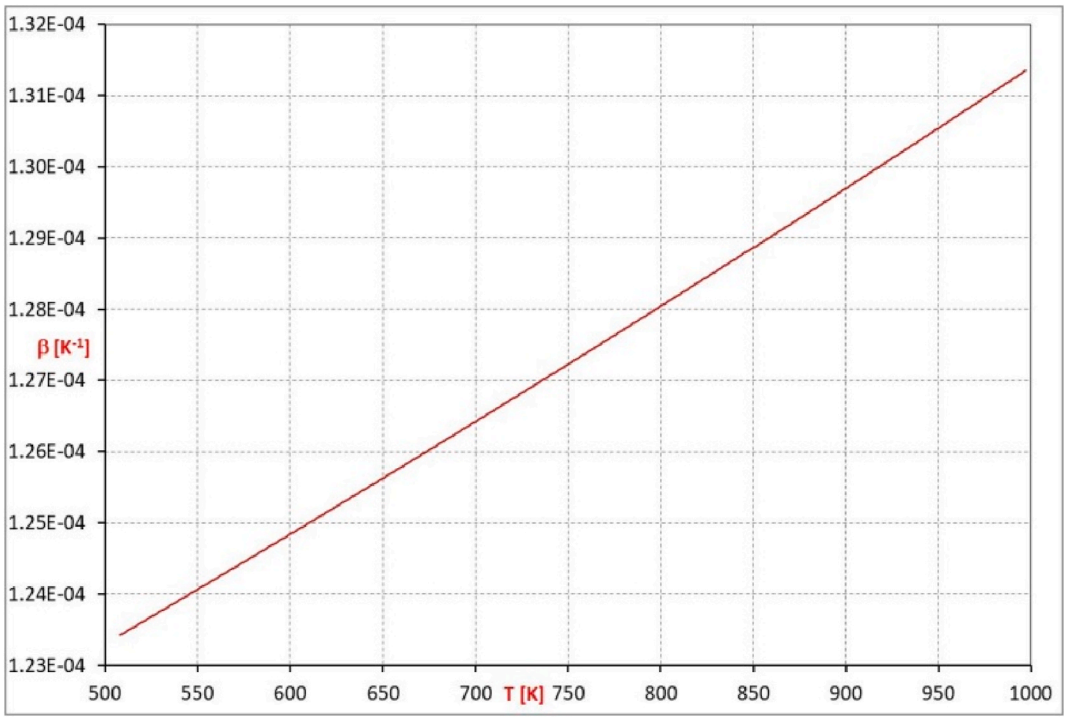

Fig. 9. Temperature dependency of the volumetric thermal expansion coefficient of the liquid Pb-Li eutectic solution.

composition, it is only necessary to perform a preliminary calibration of the system with respect to both pure Pb and pure Li, even at room temperature, to get the corresponding values of μ_i in the specific employed setup: the known density value of a pure metal at room temperature can be introduced as input parameter in equation (18) to get its value of μ_i, then the obtained μ_i values of the 2 pure metals can be introduced in equation (19) to calculate μ_{sol} and employ it all over the temperature range of interest.

The first investigation of a Pb-Li solution with the penetrating γ-rays technique was performed in 1988 by Prokhorenko [56,57], as a part of the study of the physio-chemical characteristics of the Pb-Li eutectic made at the Lvov Polytechnical Institute, even if the investigated composition actually corresponded to 17 at.% of Lithium (the old eutectic definition). Then, in 2006, Stankus [58] investigated a Pb-Li sample with the same composition, but with an improved procedure and setup, optimized particularly in terms of the sample purity; finally, in 2016, Khairulin [59], member of the same working group of Stankus, applied an even more optimized γ-ray attenuation technique to a wide range of Pb-Li solution compositions, including this time also the real eutectic one (15.7 at.% of Lithium).

Density values achieved through γ-rays technique are all rather close each other but result higher than those achieved through the other techniques [43,50,54] by about 3.0–3.5 %. Stankus [58] ascribed this discrepancy mostly to the different composition of the alloys prepared and investigated by the different authors, and to the possible existence of a gradient of concentration within the sample itself. Fig. 8 is an overview of the many experimental correlations (density vs temperature) proposed by the aforementioned authors and taken from Ref. [59]. In particular, the dependencies for the $Li_{17}Pb_{83}$ melt reported by Refs. [43,54] appear significantly lower than those obtained by Ref. [59] for the same composition; moreover they result even smaller than those reported by Ref. [34] for the composition $Li_{20}Pb_{80}$, and this anomaly (density shall increase with Pb content) led Khairulin to conclude that the data from Refs. [43,54] on the density and the thermal expansion were affected by significant errors.

The correlations obtained by Ref. [59] for the density of the eutectic solution, i.e.:

$$\rho\ [\mathrm{Kg\ m^{-3}}] = (10581.8 \pm 35.5) - (1.229 \pm 0.027) \cdot T \text{ (valid for } 508 \leq T \leq 997\ \mathrm{K}) \quad (20)$$

is considered the most accurate among all reported until now in literature. The reasons of this choice are.

1) The high accuracy in the sample preparation. Purities of the employed raw material was very high (Lead was 99.992 wt%, Li was 99.95 wt%); each sample was prepared in a glovebox filled with high-purity Argon; an electronic analytical balance was employed for the weighing process; the cell was installed in the furnace of the γ-densitometer (employing ^{137}Cs as source) avoiding the contact between sample and air, then the furnace was evacuated and filled with pure Ar up to 0.1 MPa: on the whole the uncertainty in the alloys composition was estimated to be within ±0.04 at %.
2) The homogeneity of the liquid alloy was also verified by measuring the γ-rays attenuation produced by different points of the sample, at different heights.
3) Density was measured both in isothermal conditions and in thermally dynamic experiments (founding no significant differences in the results).
4) Considering also the fair accuracy in the temperature measurement, the total relative error in density measurement was reported to be very small (≤0.2 % at 450K, ≤0.4 % at 1050K).
5) Correlation (20) is actually the only one obtained through a direct investigation of a real eutectic solution (x_{Li} = 15.7 %). So, no interpolation of experimental data achieved from different compositions must be done and no additional approximation is hence introduced in the result.

Regarding the total uncertainty of the values obtained through equation (20), it assumes the highest value in correspondence of the highest temperature (997 K): in this case it can be calculated as ~ 0.67 % in relative terms.

Table 5
Experimental α or λ vs T correlations available in literature for the Pb-Li 'near eutectic' solutions.

Author	Li content [mol %]	Method	Correlation	Range of T [K]	Ref.
Schulz	16.8	Laser flash	$\alpha\ [mm^2\ s^{-1}] = 0.13 + 0.0130\ T\ [K]$	508–623	[43]
Kondo	17.0	Laser flash	$\alpha\ [mm^2\ s^{-1}] = -10.5 + 0.0346\ T\ [K]$	573–773	[42]
Agazhanov	15.7	Laser flash	$\lambda\ [W\ m^{-1}\ K^{-1}] = 0.71 + 0.0291\ T\ [K] - 1.064 \cdot 10^{-5}\ T^2\ [K^2]$	508–1273	[61]

4.2.3. From the density to the volumetric thermal expansion coefficient

As explained in section 4.2.1, the functional correlation for the volumetric thermal expansion coefficient (β vs T) can be obtained by simply applying relation (15) to equation (20). From the general linear relation for the density:

$$\rho(T) = a - b * T \tag{21}$$

we get therefore

$$\beta = -\frac{1}{\rho}\frac{\partial}{\partial T} = \frac{b}{\rho} = \frac{b}{a - b * T} = \frac{1}{(a/b) - T} \tag{22}$$

Thus, considering the specific a and b values reported in equation (20), we get the relation:

$$\beta\ [K^{-1}] = \frac{1}{8610 - T}\ (\text{valid for } 508 \le T \le 997\ K) \tag{23}$$

which is graphically shown in Fig. 9. The expansion coefficient increases a bit with temperature, with an almost linear trend, and assumes always values of the order of $10^{-4}\ K^{-1}$.

In order to evaluate the accuracy of the β value so calculated, we must observe that it depends on the uncertainty associated to both the b term (~2.2 % according to equation (20)) and to the total ρ value (previously calculated, by excess, as 0.67 %). Therefore, if we include these uncertainty terms in equation (20), we get:

$$\beta + \Delta\beta = \frac{b\ (1\ \ 0.022)}{(1\ \ 0.0067)} = \beta\ \frac{(1\ \ 0.022)\ (1\ \ 0.0067)}{(1\ \ 0.0067)\ (1\ \ 0.0067)}$$
$$\sim\ \beta\ (1 \pm 0.022)\ (1 \pm 0.0067)\ \sim\ \beta\ (1 \pm 0.029) \tag{24}$$

Therefore, $|\Delta\beta|$ results ≤2.3 %, in relative terms.

4.3. Thermal diffusivity and thermal conductivity

4.3.1. Theoretical premise

In this section the heat transport properties of the liquid Pb-Li eutectic will be investigated, namely its thermal diffusivity and its thermal conductivity. Being 'transport properties', they are not extensive properties increasing with the amount of substance, they depend instead on the specific motion of free electrons and atoms inside the liquid structure.

Whenever a temperature gradient (→T) exists inside a material, a heat flow ($\vec{q}$) is established according to the Fourier's law, which, in case the material is homogeneous and isotropic, satisfies the relation [60]:

$$\vec{q} = -\lambda\ \vec{\nabla} T \tag{25}$$

Accordingly, thermal conductivity, λ [W m^{-1} K^{-1}], is defined as the heat that flows in unit time through a unit area of a layer of material with unit thickness, in response to a unit temperature difference.

The heat flow through the material produces in turn a temperature change in each specific point of its; the temperature evolution, both along the space and the time coordinates, is described by the differential equation of the heat conduction [61]:

$$\nabla^2 T - \frac{1}{\alpha}\frac{\partial T}{\partial t} = 0 \tag{26}$$

where α [$m^2 s^{-1}$] is the thermal diffusivity of the material.

Thermal conductivity and thermal diffusivity anyway are not independent quantities, but it is possible to verify that they are linked by the relation below [60],

$$\lambda = \alpha \cdot c_p \cdot \rho \tag{27}$$

indicating that thermal conductivity of a system corresponds to its thermal diffusivity multiplied by its density (ρ) and its specific heat (c_p) (the product $c_p \cdot \rho$, [J m^{-3} K^{-1}], is also called '*volume heat capacity*'). For this reason, being the 2 thermal quantities a different representation of the same physical property, it makes sense in this section to treat them together and link them through the correct correlations for c_p and ρ already selected in this document, this way assuring the internal coherence of all of them.

4.3.2. Experimental diffusivity and conductivity data from literature

Due to the complexity of the theoretical description of the physical mechanisms affecting the heat transport properties, reliable values of the heat conductivity and diffusivity can be achieved only through experimentation. Anyway, there is an intrinsic complexity also in the experimental investigations, since transport properties are asked to describe systems that are not in an equilibrium state; additionally, when the heat flux must be measured at high temperature, as is the case of many liquid metals and metallic alloys, the inaccuracy of the result may become significant, because of the heat losses associated to radiation and convective transfer from the sample to the environment. Consequently, data reported by different authors are often so incongruous to overstep the possible total errors estimated by each of them, and the coefficients of variation with temperature sometimes assume even opposite signs.

Three independent, experimental works [42,43,61] are reported in literature for the determination of the thermal diffusivity and conductivity of the liquid Pb-Li eutectic; their outcome is summarized in Table 5. They are all based on the laser flash method, even if employing a different setup and a different calculation model to extract from the output of the analysis (a temperature vs time diagram) the correct thermal properties of the system. Additionally, other data for the Pb-Li thermal properties can be found in Ref. [40], but they do not come from real measurements and are instead only calculated through the additivity rule, i.e. by adding the corresponding properties of the two pure metals constituting the eutectic, each one weighted by its atomic concentration: this approach is quite misleading and will not be considered here.

Schulz [43], in 1986, investigated a Pb-Li sample prepared as already described in the Specific Heat and Density sections of this document, i.e. characterized by a Li content equal to ~0.67 wt% (16.8 at.%) and prepared under Argon atmosphere starting from 99.4 % purity Li and 99.9 % purity Pb. He covered the sample (cylindrical shaped) with CaF_2 discs on both sides, allowing the absorption of the laser flash (wavelength 1.06 μm) on the front one and registering the temperature rise at the rear one, with an In-Sb Infrared Detector (IR). He calculated at first the thermal diffusivity, then, exploiting equation (27) and the expressions he had already found for the specific heat and the density, he got the conductivity.

Several weaknesses can be found in Ref. [43] experimentation: the Pb-Li sample composition, which does not match the correct eutectic one; the range of investigated temperatures, 513–623K, which is rather

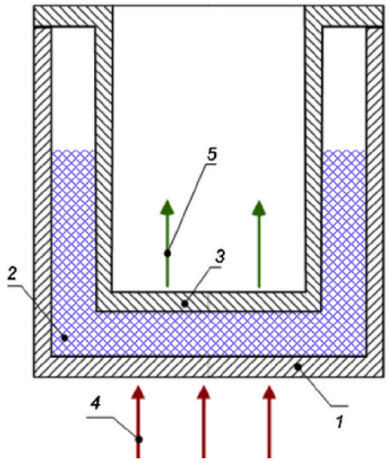

Fig. 10. Scheme of the measuring ampoule in the Agazhanov experiment: 1 = steel crucible; 2 = liquid sample (Pb-Li); 3 = steel lid; 4 = laser pulse; 5 = detected infrared radiation*
* Reprinted from Fusion Engineering and Design, 152, A.Sh. Agazhanov et al., Thermal conductivity and thermal diffusivity of Li-Pb eutectic in the temperature range of 293–1273K, 111456, Copyright (2020), with permission from Elsevier.

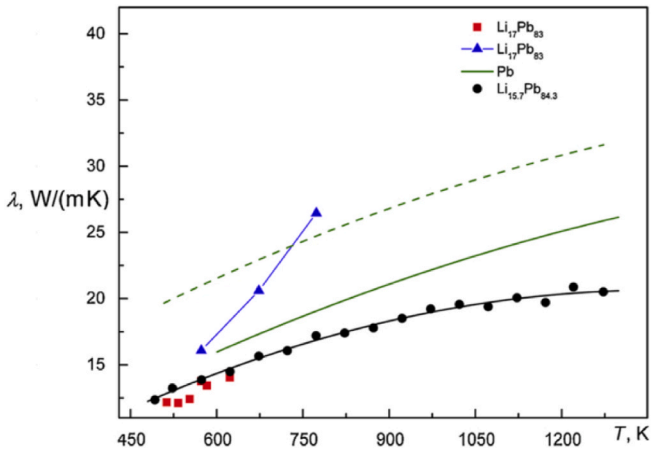

Fig. 11. Liquid phase thermal conductivity of eutectic and near-eutectic alloys. Black points and fitting curve are data from Agazhanov [61]; red squares are data from Schulz [43]; blue triangles/fitting curve are data from Kondo [42]; dashed green curve is calculated through the additivity rule; solid green line is, for comparison, thermal conductivity of pure Lead [66]*
* Reprinted from Fusion Engineering and Design, 152, A.Sh. Agazhanov et al., Thermal conductivity and thermal diffusivity of Li-Pb eutectic in the temperature range of 293–1273K, 111456, Copyright (2020), with permission from Elsevier.

narrow, raising some doubt about the accuracy of values obtainable by extrapolation at higher temperatures; the calculation model adopted, which is not described in the paper, where only the std deviation of obtained values is actually indicated (≤5 %); finally, the fact that the same procedure, previously applied by the same author to a pure Lead liquid sample, had produced thermal diffusivity values up to 20 % higher than those already reported for Lead by Touloukian [62], so no confirmation of the method soundness can be given by any comparison with previous independent measurements.

Later, in 2016, Kondo [42], using a ULVAC TC-9000 device, investigated three different Pb-Li samples, characterized respectively by a Li molar fraction equal to 5, 11 and 17 at.%, in order to evaluate the effect of the composition on the value of the thermal diffusivity. Each Pb-Li sample was fabricated by the author using small grains of Pb and Li at 723K; Li concentration in the samples was determined by measuring its melting points and through the ICP-AES analysis. The sample, shaped as a disk with diameter smaller than 9 mm and thickness of 1 mm, was placed inside a graphite holder, between 2 sapphire plates, and heated. Operating under a pressure of 1 Pa, a Nd glass laser (wavelength = 1.07 μm, pulse duration = 0.49 ms, energy output = 10 J)[3] irradiated the top surface of the sample and the temperature increase of the opposite one was measured by an infrared detector. Thermal diffusivity of the sample was evaluated by applying the adiabatic model proposed by Parker [63], particularly its equation (7).

The working procedure performed by Kondo has some strong points with respect to Schulz one, in that it covers a wider temperature range (up to 873K) and its description is more detailed, in particular regarding the calculation model and the observation about the thermal convection in the thin Pb-Li liquid film,. Yet, even the work of Kondo presents some weaknesses: none of the examined Pb-Li samples has a composition actually matching the real eutectic one (15.7 at.% of Li); according to the observations made by Ref. [61], the sapphire plate might have absorbed a bit of the infrared radiation, hence affecting the signal received by the IR detector; finally, the heat losses to the environment, not negligible at the experiment temperatures, could have made the employed Parker model a bit inaccurate.

By comparing the results achieved by Kondo with those by Schulz, the former are always higher, up to about 40 % more (at 623K) of the latter, and some doubt remains about the correctness of both the experimentations.

More recently (2020), a new measurement of liquid Pb-Li thermal properties has been executed by Agazhanov [61] and led to a better description of the system of our interest. Here, the investigated sample was characterized by a composition matching the real eutectic one (Li = 15.7 at.%). The eutectic mixture was prepared starting from 99.992 wt %. purity Lead and 99.95 wt% purity Lithium; the metals, preliminarily cleaned from surface oxide films and handled under a protective Argon atmosphere inside a glovebox, were then melted together inside a special steel tube, twice increasing the temperature up to 900K.

The methodology employed by Agazhanov [61] is based again on the laser flash irradiation of the sample, but it resorts to a different experimental setup and particularly a different calculation model, already presented in Refs. [64,65]. Agazhanov used a sealed steel cylindrical ampoule (Fig. 10), in which the liquid sample (indicated as '2' in the figure) was 'clamped' between the crucible ('1') and the lid ('3'). The design of such an ampoule provides a plane-parallel liquid layer of known thickness and a good contact between the sample and the bounding surfaces. A laser pulse ('4') is supplied to the bottom surface of the crucible, generating a heat flux directed upward, which crosses the crucible itself, the sample layer and the lid; radiation from the upper surface of the lid ('5') is finally received by an infrared detector and then converted into an electrical signal.

In order to get, from the output of the experiment (the measured temperature), the thermal diffusivity and conductivity of the liquid Pb-Li sample, equation (26) was solved in cylindrical coordinates (r = distance along the radius of the ampoule; z = vertical direction): this required to properly fix the boundary conditions, as detailed by relations (3) to (13) in Ref. [61]. In this set of relations, it can be noted: the emission from the external surfaces of the ampoule was taken into account too, through the introduction of the parameter ε (emissivity factor); density and specific heat values of both phases (steel and liquid

[3] In laser flash procedures the pulse is very short and the transferred energy is consequently small, in order to make small the temperature increase of the sample: this way it is possible to assume the consistency of the sample thermal diffusivity during each single experiment. The variation of the diffusivity value with temperature is instead assessed by comparing the results achieved in different experiments, characterized by quite larger differences in the starting operating temperature.

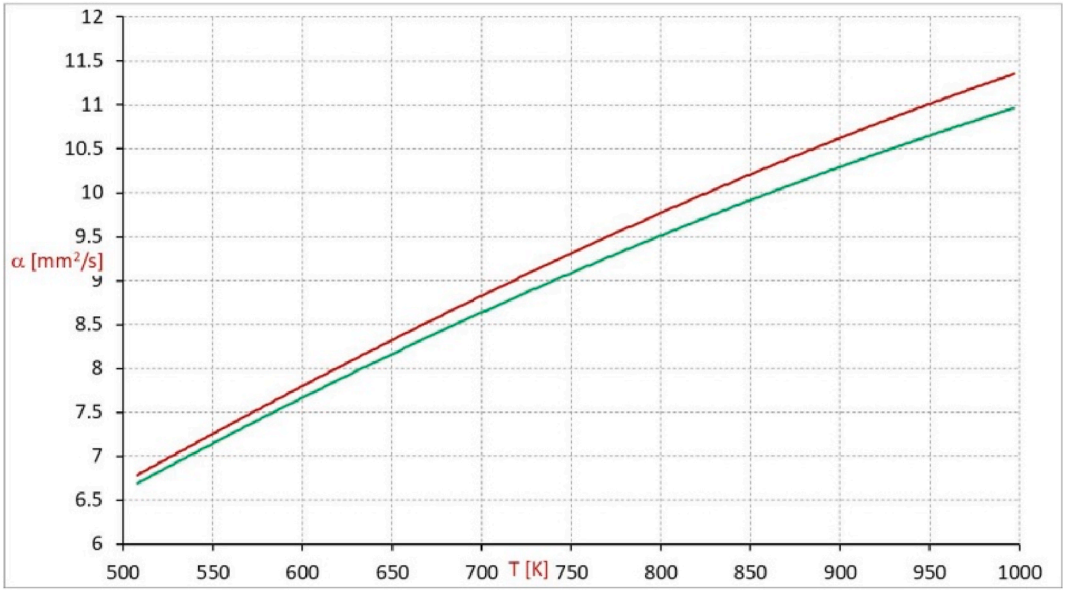

Fig. 12. Liquid phase thermal diffusivity of the eutectic Pb-Li alloy. Green curve is the plot of the original equation proposed by Agazhanov [61]; red points and fitting curve have been instead calculated here starting from equations ((10), (20), (27) and (28).

Pb-Li eutectic) were taken from previous literature data and inserted as known values in the equations, and they affected the heat propagation at each interphase; the change in the Pb-Li liquid layer thickness was considered as well, through the thermal expansion of the ampoule material.

The thermal conductivity of liquid Pb-Li was hence determined, at each investigated temperature, by the best agreement (root-mean-squared deviation) between the experimental heating thermogram and the one calculated solving the abovementioned equation: the thermal conductivity of Pb-Li and the emissivity factor of the steel were the 2 real fitting parameters of this calculation.

From the values found for the thermal conductivity (λ), the following fitting correlation was constructed:

$$\lambda\ [\mathrm{W\ m^{-1}\ K^{-1}}] = 0.71 + 0.0291\ \mathrm{T} - 1.064 \cdot 10^{-5}\ \mathrm{T}^2 \quad (28)$$

(valid in the range $508 \leq \mathrm{T} \leq 1273\mathrm{K}$)

It must be said that in his calculation Agazhanov employed, as known values for the density and the specific heat of the liquid eutectic Pb-Li, those coming respectively by equation (20) [59] and equation (9) [43] of this paper. While the first equation has been actually evaluated as the best one for the density of the eutectic (see section 4.2.2), equation (9) for the specific heat was shown instead to have some limits, particularly regarding the Pb-Li composition, and the new equation (10) was therefore suggested in place of it (see section 4.1.3). Therefore, the result found by Agazanov could be a bit affected by the use of inaccurate numbers for the specific heat; anyway, he admitted an error of about 4–6% in its conductivity values (the error is higher at higher temperature), and stated that it was due mainly to the uncertainty in the properties of the ampoule material and in the Pb-Li specific heat. We think that this estimated range of error is able to include also the small discrepancy between equation (9) and equation (10), so we keep his estimation.

Fig. 11 shows thermal conductivity results achieved by Agazhanov, compared with the previous, already mentioned, ones of Schulz [43] and Kondo [42], together with the data of pure liquid Lead [66] and those calculated for the eutectic solution according to the additivity rule (weighted average of the 2 pure metals). It can be verified that data from Agazhanov are indeed rather close to those of Schulz, while they are smaller than Kondo ones, particularly the higher is the temperature. It's also worth noting that the addition of 15.7 at.% Li to pure Pb does not increase the thermal conductivity, as it would be expected if the simple additivity rule held: all Agazhanov eutectic data lie in fact below pure Pb ones and, even more, below pure Li ones (thermal conductivity of pure Li [67] is higher than Pb one). Such conductivity behaviour, which may appear strange, can be explained remembering (see section 2.3) that the liquid Pb-Li system is far from being an ideal solution, and that the valence electrons of the metals (main responsible for the heat conduction) are less free to move than in pure metals, being partly localized in ionic type interatomic bonds. It is for this same reason that, as will be seen in section 4.4, electrical conductivity of liquid Pb-Li eutectic is smaller than those of pure constituting metals: also this property is dependent in fact on the electrons motion throughout the phase.[4] This coherence between the behaviours of thermal and electrical conductivity is another point that makes Agazhanov results stronger than Kondo ones.

For what concerns the selection of a suitable correlation for the thermal diffusivity of the liquid Pb-Li eutectic, we don't choose here the one suggested by Agazhanov, since we know it is related to thermal conductivity one through the employment of an inaccurate Specific Heat correlation. Therefore, to keep the coherence of all the correlations till now proposed in this paper, thermal diffusivity values have been here calculated at each temperature employing equations ((10), (20), (27) and (28); from the fitting of the obtained values, the new relation is proposed:

$$\alpha\ [\mathrm{mm^2\ s^{-1}}] = 0.208 + 0.0160\ \mathrm{T} - 4.405 \cdot 10^{-6}\ \mathrm{T}^2 \quad (29)$$

This relation is considered to hold from the eutectic melting point up to 997K, i.e. in the range of temperature for which all the employed equations, (10), (20) and (28) are considered valid. The relative uncertainty associated to the diffusivity values is considered at most equal to 7 %, i.e. the value obtained by summing, under square root, the squares of the maximum uncertainties associated to the 3 above equations.

Fig. 12 plots, in red, the calculated thermal diffusivity values, which are coincident with their fitting red curve (the above equation), since

[4] According to the Wiedemann-Franz law, the ratio between the thermal and electrical conductivity of a metal is proportional to the temperature; moreover, the proportionality constant (Lorenz number) assumes values almost equal in different metals. This aspect will be dealt in detail in section 4.4.3.

Table 6
Experimental ρ_{el} vs T correlations available in literature for the Pb-Li 'near eutectic' solutions.

Author	Li content [mol %]	Method	Correlation	Range of T [K]	Ref.
Schulz	16.8	4 points Thomson bridge	ρ_{el} [μΩ cm] = 102.3 + 0.0426 T [K]	508–933	[43]
Hubberstey	16	Electrical Resistivity Monitor	ρ_{el} [μΩ cm] = 101.26–4.982 · 10^{-3} T [K] + 4.095 · 10^{-5} T^2 $[K]^2$	600–800	[71]
Hubberstey	17	Electrical Resistivity Monitor	ρ_{el} [μΩ cm] = 103.33–6.750 · 10^{-3} T [K] + 4.180 · 10^{-5} T^2 $[K]^2$	600–800	[71]
Hubberstey	18	Electrical Resistivity Monitor	ρ_{el} [μΩ cm] = 105.40–8.461 · 10^{-3} T [K] + 4.267 · 10^{-5} T^2 $[K]^2$	600–800	[71]

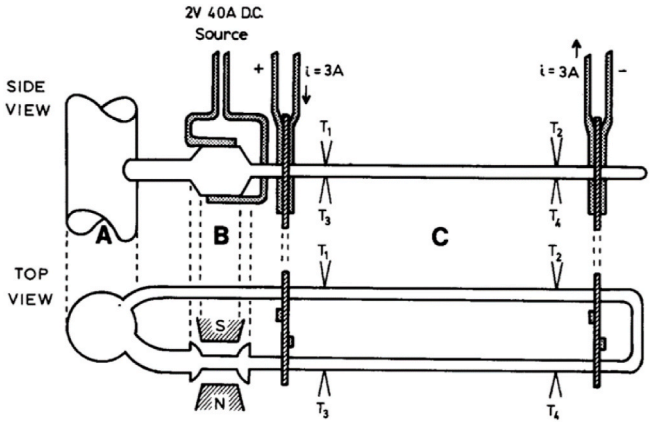

Fig. 13. Sketch of the resistivity monitor employed by Hubberstey. A: bulk Pb-Li source; B: miniature electromagnetic pump; C: capillary section*
* Reprinted from Fusion Engineering and Design, 14, P.Hubberstey et al., An electrical resistivity monitor for the detection of composition changes in Pb-17Li, 227–233, Copyright (1991), with permission from Elsevier.

data were extremely correlated ($R^2 = 0.9999$). Green curve is instead the plot of the original equation proposed by Agazhanov for the thermal diffusivity: it's easy to see that the distance between the curves is always small, in relative terms, up to a max of 3.4 % at 997K. Green curve lies below the red, correct one, since Agazanov, in his calculation, over-estimated the specific heat of the liquid Pb-Li eutectic.

4.4. Electrical resistivity

4.4.1. Theoretical premise

Electrical resistivity (ρ_{el}; the subscript '*el*' is employed in this paper to distinguish it from the symbol of density, ρ) is the inverse of electrical conductivity (σ), therefore is a 'transport property' of the material. As such, it is not an extensive property which increases with the amount of substance and it is not possible to simply evaluate it from the knowledge of the resistivity of the pure components.

A parallel exists anyway between thermal and electrical conductivities. Electrons movement throughout the material is in fact responsible for both its electrical and its thermal conductivity, even if for the latter a minor, additional 'lattice' contribution is also present. The existence of this common dependence permits to relate thermal and electrical transport properties, and will be employed in section 4.4.3 to verify the internal coherence of the correlations selected to describe the 2 transport mechanisms.

It must be also reminded here that, according to Matthiessen's rule [68], electrical resistivity of metals is generally composed of 2 parts: the residual resistivity, ρ_0, which does not depend on temperature, and the intrinsic resistivity, ρ_1, which instead increases rapidly with temperature. In math terms:

$$\rho_{el}(T) = \rho_0 + \rho_1(T) \tag{30}$$

While ρ_0 arises from the electrons interaction with chemical and physical imperfections of the metal, ρ_1 is instead due to the interactions with phonons, i.e. the lattice vibrations which are, of course, dependent on temperature.

Table 7
A, B and C fitting parameters of equation (32), at several temperature values[a].

T [K]	A	B	C
623	96.37	0.905	0.0124
648	97.43	0.934	0.0112
673	98.53	0.961	0.0099
698	99.60	0.995	0.0085
723	100.67	1.042	0.0067
748	101.73	1.095	0.0047
773	102.79	1.148	0.0028

[a] Reprinted from Fusion Engineering and Design, 14, P.Hubberstey et al., An electrical resistivity monitor for the detection of composition changes in Pb-17Li, 227–233, Copyright (1991), with permission from Elsevier.

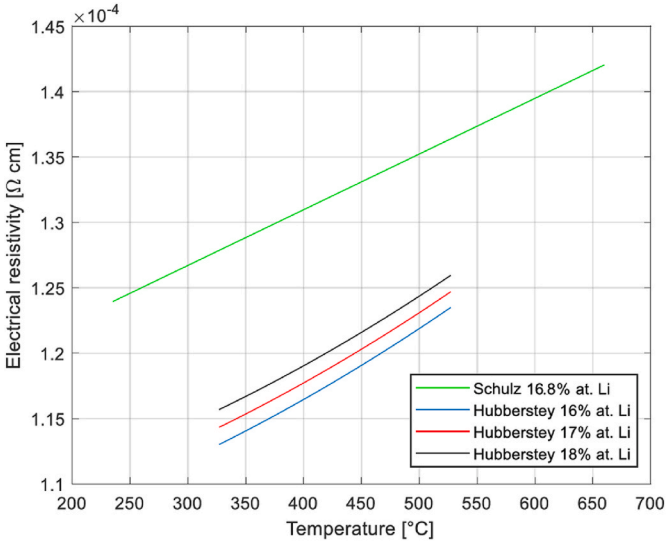

Fig. 14. Plot of the electrical resistivity of Pb-Li near eutectic alloys, according to Schultz [43] and Hubberstey [71] works*
* Reprinted from Fusione Engineering and Design, 138, D.Martelli et al., Literature review of lead-lithium thermophysical properties, 183–195, Copyright (2019), with permission from Elsevier.

4.4.2. Experimental resistivity data from literature

Only 2 different experimentations have been reported so far in literature, focused on the accurate determination of the electrical resistivity values of the eutectic (or near eutectic) Pb-Li liquid solution; their outcome is summarized in Table 6. It is true that Nguyen in 1977 [69] and Meijer in 1985 [70] investigated the electrical transport properties of Pb-Li solutions characterized by several compositions, so to construct resistivity vs composition graphs, anyway none of them was precisely corresponding to the real eutectic one, moreover resistivity values were reported at a single, fixed, temperature. Therefore, only in the later works of Schulz [43] and Hubberstey [71] it is possible to find a correlation describing the variation of the eutectic electrical resistivity with temperature.

Schulz [43], in 1986, investigated a Pb-Li sample prepared as already described in other sections of this document (4.1.2,4.2.2 and 4.3.2), i.e.

Table 8
Electrical resistivity values of a real eutectic solution ($x_{Li} = 0.157$) calculated at several temperatures on the basis of Hubberstey experimental data.

T [K]	623	648	673	698	723	748	773
ρ_{el} [μΩ cm]	113.63	114.85	116.06	117.32	118.68	120.09	121.50

characterized by a Li content equal to ~0.67 wt% (~16.8 at.%) and prepared under Argon atmosphere starting from 99.4 % purity Li and 99.9 % purity Pb. A four points Thompson bridge was employed to measure the electrical resistivity; the experiment was conducted in vacuum condition, and the thermal expansion of the Pb-Li solution was taken into account to calculate the correct sample size. No other details are reported in the paper, nor pictures of the employed setup.

From the plot of the resistivity versus temperature values, Schulz proposed the following correlation for the liquid Pb-Li solution (Li = 16.8 at.%):

$$\rho_{el}\ [\mu\Omega\ cm] = 102.3 + 0.0426\ T \quad (31)$$

(valid for $508 \leq T \leq 933$ K)

It is not clear why the author indicates as 933K the maximum temperature value for the equation validity, considering that in his plot an experimental point at ~ 975K is present too. According to him, the accuracy of the results corresponds to ±5 %.

The other relevant work in this field is the one made by Hubberstey [71]. For the measurement he employed a resistivity cell originally conceived at Nottingham for the study of the chemistry of liquid metal solutions [72], whose sketch is shown in Fig. 13.

Without entering too many details of this device, which can be retrieved in the original papers, it must be observed that the sample electrical resistance is determined by a version of the four-terminals method, by measuring the electrical potential difference created across 2 silver plates; these plates are joined to the capillary tube in which the liquid Pb-Li flows, being pushed by the miniature electromagnetic pump. It is hence clear that the resistance values so obtained do not reflect only the properties of the flowing liquid metal, but also of the steel the capillary section is made of. Therefore, being the external steel and the inner Pb-Li 2 parallel conductors, a preliminary measurement of the empty capillary resistance must be executed at each investigated temperature, in order to get, through the expressions for the sum of parallel resistances, the Pb-Li alone value. According to the author, the device was characterized by a sensitivity of ~0.6 nΩm and the accuracy in the temperature regulation was ±0.5 K.

Regarding the Pb-Li solutions, they were prepared starting from 99.999 % pure Lead and 99.8 % pure Lithium; several composition were investigated, starting from 100 % Lead and adding, progressively, small aliquots of Lithium, up to a maximum of 20.5 at.% of Lithium. For each composition, a resistivity vs temperature was constructed, up to 800K. Additionally, the general isotherm resistivity-composition relation was inferred,

$$\rho_{el}\ [\mu\Omega\ cm] = A(T) + B(T) \cdot x_{Li}\ [at.\%] + C(T) \cdot (x_{Li}\ [at.\%])^2 \quad (32)$$

where A, B and C are parameters which vary with temperature. From the fitting of the experimental points, the values of A, B, and C at several temperatures were calculated: they are reported in Table 7.

Employing the above values and applying equation (32) to Pb-Li composition respectively equal to 16, 17 and 18 at.% Li, it was possible for Hubberstey to calculate the trend with temperature of the electrical resistivity of these 3 near eutectic solutions. They are reported in Table 6 and shown also in Fig. 14, together with the plot of the already mentioned Schulz equation (31).

Curves in Fig. 14 indicate.

- resistivity values calculated by Hubberstey increase with the Lithium content in the alloy, and they are even higher than pure Pb resistivity at the same temperature (and even more than pure Li one), as can be simply verified by putting $x_{Li} = 0$ in equation (32). This fact, apparently strange, agrees anyway with the already discussed non-ideality of the Pb-Li liquid solutions: due to the existence of some structural order inside the solution and to the partial ionic nature of the hetero-atoms interactions, conduction electrons are less free to move than in the pure metals and remains somewhat localized. Additionally, this experimental evidence agrees also with the behaviour of the thermal conductivity of the Pb-Li eutectic solution, since its description through equation (28) led for the same reason to values smaller than pure Pb and pure Li conductivities (see again Fig. 11).
- Schulz values are higher than Hubberstey ones at the same temperature, the difference largely exceeding the possible composition effect. The trend with temperature of Schulz curve is not too different from those of Hubberstey curves (even if Hubberstey values increase a bit more with temperature, due to the existence of a positive second order term), but there is an additional positive contribution in Schulz resistivities that shift up his curve by almost 10 % in relative terms.

After all these considerations, we don't dispose anyway of so many info and elements to indicate with certainty which of the 2 experimental set of data shall be considered more trustable. Actually, later experimentations performed by different authors with a resistivity monitor device similar to the one employed by Hubberstey [73], have indicated some intrinsic limits of this measurement procedure, like for instance the influence on the result of possible parasitic currents originated by the mini electromagnetic pump, of the not homogeneous temperature distribution inside the measurement capillary, …Nonetheless, for the moment, it seems preferable to rely on the work made by Hubberstey, because it was more deeply described and it was based on the acquisition of many more resistivity values, at several temperatures and compositions, showing, if nothing else, a good reproducibility and internal coherence of the results.

Moreover, the work made by Hubberstey gives also the possibility to adapt the general equation (32) to a Pb-Li liquid solution characterized by a composition exactly matching the eutectic one, i.e. $x_{Li} = 0.157$. In fact, if we put in equation (32) $x_{Li} = 0.157$ and, for each temperature value, the A,B and C parameters reported in Tables 7 and it is possible to calculate the corresponding electrical resistivities of our solution of interest: they are reported in Table 8 (this calculation procedure is actually the same adopted by Hubberstey for the solutions characterized by $x_{Li} =$ 0.16, 0.17 and 0.18).

The fitting of Table 8 values leads to the following (ρ_{el} vs T) equation:

$$\rho_{el}\ [\mu\Omega\ cm] = 101.28–6.380 \cdot 10^{-3}\ T + 4.211 \cdot 10^{-5}\ T^2 \quad (33)$$

which is characterized by a R^2 correlation coefficient equal to 0.99996 and it's valid in the range 600–800 K (range of the experimental points employed to construct it). Unfortunately it is not possible to associate to this equation an intrinsic accuracy, because it follows from on the original experimentation made by Hubberstey, who only declared the maximum admitted temperature uncertainty (±1K), but didn't evaluate all the possible sources of errors and of their propagation.

In any case, equation (33) is considered, for the moment, the most suitable to describe the electrical resistivity of the liquid Pb-Li eutectic solution. It is not graphically represented here, but it's easy to see that it will be substantially parallel to Hubberstey curves shown in Fig. 14, and just a bit below the blue one.

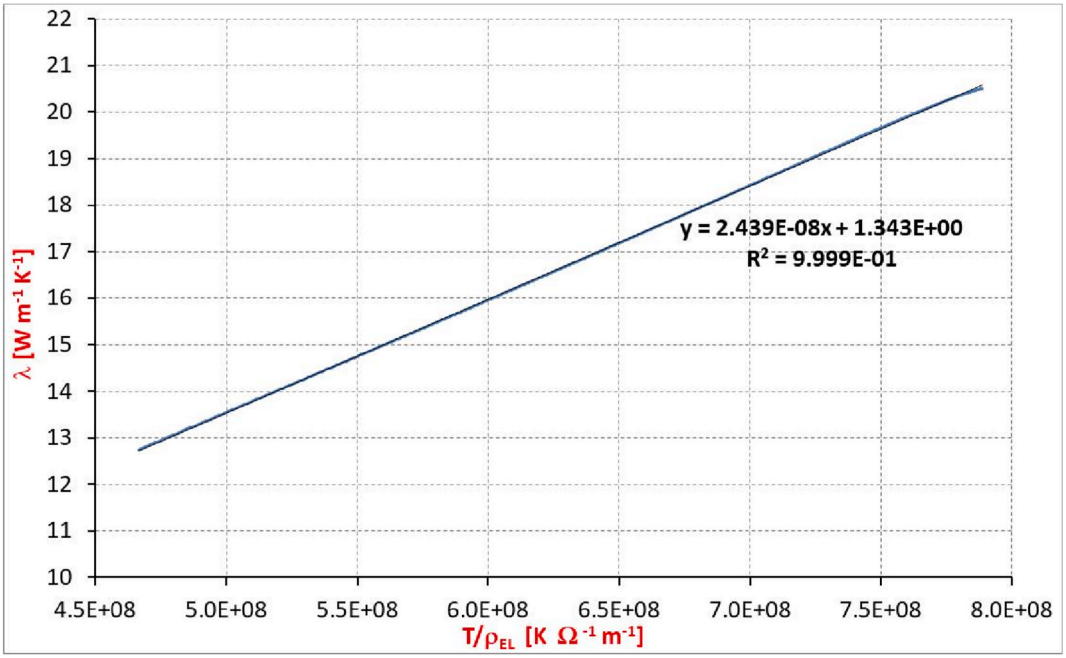

Fig. 15. Plot of λ(T) vs $\left(\frac{T}{\rho_{el}(T)}\right)$ calculated according to equations (28) and (33) in the range 508–1273 K.

4.4.3. Cross-check of thermal and electrical conductivity correlations

As anticipated in section 4.4.1, thermal and electrical (σ) conductivities of a metal are strictly correlated, since both of them are dependent on the electrons mobility inside the material. In this regard, Wiedemann and Franz [74] in 1853 formulated an empirical law relating the thermal and electrical conductivities of a metal, stating that the ratio of the electrical and thermal conductivities (*WF ratio*) at a given temperature is approximately the same for all the metals. In 1872 Lorenz discovered that the WF ratio is also proportional to the temperature.

Later, it was evidenced that the thermal conductivity it is actually composed of 2 contributions: the lattice contribution λ_L, originated from the phonons transport, and the electronic contribution λ_E, originated from the electrons/holes transport:

$$\lambda = \lambda_L + \lambda_E \tag{34}$$

Therefore, only λ_E (not the full λ) is to be correlated with σ and the Wiedemann-Franz hence becomes:

$$\frac{\lambda_E}{\sigma} = \lambda_E \cdot \rho_{el} = L \cdot T \tag{35}$$

where L [$V^2\ K^{-2}$] is defined as the Lorenz number. The total expression for the thermal conductivity is therefore:

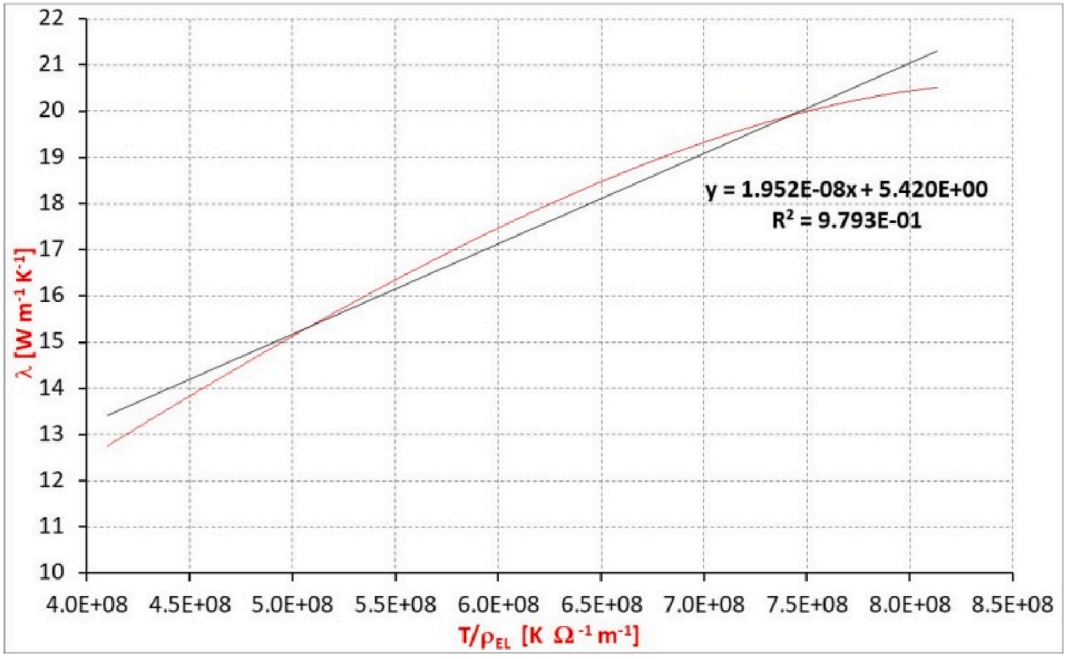

Fig. 16. Plot of λ(T) vs $\left(\frac{T}{\rho_{el}(T)}\right)$ calculated according to equations (28) and (31) in the range 508–1273 K.

$$\lambda = \lambda_L + \frac{L \cdot T}{\rho_{el}} \quad (36)$$

Sommerfeld [75] calculated the first order approximation of L from the free electrons theory of metals, obtaining as result the value:

$$L_0 = \frac{\pi^2}{3}\left(\frac{k_B}{e}\right)^2 = 2.443 \cdot 10^{-8}\ V^2\ K^{-2} \quad (37)$$

In the above expression, Sommerfeld number is indicated as L_0 to distinguish it from a generic L value satisfying equation (35); k_B is the Boltzmann constant; e is value of the electric charge of the electron.

Regarding equation (34), it must be observed that the electronic contribution (λ_E) to the thermal conductivity is predominant in an almost all the metals, with the lattice one usually smaller than 5 % of the total; only in few cases (for instance metallic alloys at very low temperatures) the lattice transport can become important as much as the electronic one, and even more [68]. The lattice term depends on temperature, anyway it has been evidenced to become constant above the Debye temperature [76,77]; for pure liquid metals, it would correspond generally to around 1 % of the total thermal conductivity [78]. Even regarding the generic value of L of equation (36), many authors reported numbers which are a bit different from the Sommerfeld one (L_0), slightly varying with the temperature and the nature of the metal, especially in case of a metallic alloy. On the whole, anyway, the Wiedmann-Franz law was reported to hold for liquid metallic alloys, which is our situation [79].

It is now interesting to verify if the specific equations we have selected in this paper for the description of the thermal and electrical conductivities of the liquid Pb-Li eutectic solution agree somehow with the above theoretical considerations.

For the thermal conductivity we have selected equation (28):

$\lambda\ [W\ m^{-1}\ K^{-1}] = 0.71 + 0.0291\ T - 1.064 \cdot 10^{-5}\ T^2$ (valid in the range $508 \leq T \leq 1273K$)

while for the electrical resistivity we have proposed equation (33):

$\rho_{el}\ [\mu\Omega\ cm] = 101.28 - 6.380 \cdot 10^{-3}\ T + 4.211 \cdot 10^{-5}\ T^2$ (valid in the range $600 \leq T \leq 800K$)

Applying equation (28) we now calculate the values of λ at each temperature value from 508K up to 1273K; similarly, applying equation (33), we calculate all the values of ρ_{el} in the same temperature range; finally, in Fig. 15, we plot $\lambda(T)$ vs $\left(\frac{T}{\rho_{el}(T)}\right)$ for each temperature value. Calculated points are plotted in blue in the figure; they actually overlap with the fitting line (in black), which is in fact characterized by an excellent correlation coefficient ($R^2 = 0.9999$).

The black fitting line equation results:

$$\lambda\ \left[W\ m^{-1}\ K^{-1}\right] = 1.343 + 2.439 \cdot 10^{-8} \cdot \frac{T\ [K]}{\rho_{el}[\ m]} \quad (38)$$

If we compare it with the previous equation (36),

$$\lambda = \lambda_L + \frac{L \cdot T}{\rho_{el}} \quad (36)$$

we have the possibility to get the value of L ($=2.439 \cdot 10^{-8}\ V^2\ K^{-2}$) and λ_L ($=1.343\ Wm^{-1}K^{-1}$) of our system. The value of L results incredibly close (we can also say coincident!) to the theoretical L_0 calculated by Sommerfeld and reported in relation (37) ($L_0 = 2.443 \cdot 10^{-8}\ V^2\ K^{-2}$). It is quite comforting that 2 experimental relations, asked to describe 2 different transport properties, and achieved independently by different authors on the basis of different methods and setups, give at the end a so coherent description of the same system. This excellent agreement surely strengthen the soundness of each of the 2 relations.

Regarding the value obtained for λ_L, $1.343\ Wm^{-1}K^{-1}$, this constant term gives therefore a minor contribution to the total thermal conductivity, ranging from ~10 % (at the lowest temperature) to ~ 7 % (at the highest one). Its value is qualitatively reasonable, since we know that the lattice contribution generally constitutes a minor contribution with the respect to the electronic contribution.

Finally, as countercheck, we apply again the same calculation procedure employed to get the value of L and λ_L, but using, instead of equation (33), the already discussed Schulz correlation for the electrical resistivity (31): the calculated points are shown in red in Fig. 16, together with their fitting line (black).

In this case, it can be verified that the red points are not characterized by a good linear trend, in fact the value of R^2 is 'only' 0.9793. The resulting value of L here is $1.952 \cdot 10^{-8}\ V^2\ K^{-2}$ (which is much more different from L_0 than in the previous calculation) and the resulting value of λ_L ($=5.420\ W\ m^{-1}\ K^{-1}$) would indicate the lattice contribution constitutes from 26 % to 42 % of the total thermal conductivity, which seems too much.

Similarly, it can be verified that, applying (31) for the determination of the electrical resistivity and employing instead a relation for the thermal conductivity different from (28), the calculated values of L and λ_L are not able to properly define a linear trend for the fitting equation (34), and are both farther from those theoretically expected.

At the end we can hence conclude that the 2 relations (28) and (33), that were independently recognized as the most accurate for the description respectively of the thermal conductivity and the electrical resistivity of the liquid eutectic alloy, are also the ones able to assure the best internal coherence, on the basis of the theoretical knowledge of the transport properties inside a metallic alloy.

4.5. Sieverts' constant of hydrogen

4.5.1. Theoretical premise

4.5.1.1. Definition. Solubility of a gas in a liquid increases with its pressure; when the resulting concentration in the liquid phase is small and in the assumption of no chemical interaction, solubility results proportional to the pressure in the gas phase, according to the Henry's law. When the gas is diatomic, its dissolution may also entail the decomposition in its atomic constituents, provided these can be stabilized by the liquid solvent. This is the case of gas like H_2 in most liquid metals and alloys, where the generated H atoms are stabilized in the solvent by their capability to withdraw electronic density from the less electronegative solvent atoms (actually, when the concentration of solved H becomes too high, it is also possible to get the formation of a solid, separate metal-hydride phase; for instance, in liquid Lithium at 200 °C, LiH precipitation takes place for Hydrogen concentration higher than 437 appm [80]).

It is possible to formally split the dissolution process of Hydrogen inside a liquid metal (LM) in 2 separate steps, the first related to the solubilisation of the diatomic molecule as such and the second related to decomposition of the solved molecule, as below:

$$H_2(g) + n\ LM \rightleftharpoons H_2(sol) \rightleftharpoons 2H(sol) \quad (39)$$

where (g) and (sol) denote, respectively, the gaseous and the liquid solution phases, and n is a generic coefficient (not necessary an integer number) which defines the solvation sphere in the liquid phase. The constant, K_{SOL}, which regulates the overall dissolution equilibrium, is hence:

$$K_{SOL} = \frac{a^2_{H\ (sol)}}{P_{H_2}\ a^n_{LM}} \quad (40)$$

where a_x is the activity of the x species in the liquid solution phase and P_{H_2} is the Hydrogen pressure in the gas phase. In the above equation, the activity of the liquid metal (a_{LM}) can be set as 1, being the dissolved

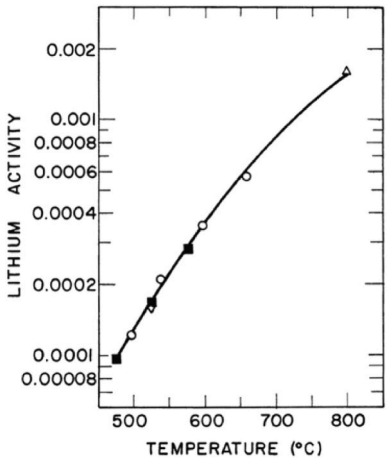

Fig. 17. Lithium activity for the 'near eutectic' $Li_{17}Pb_{83}$ solution according to the experimental works of several authors: ○ [19], ▽ [82], Δ [83], ▮ [84].

hydrogen a very minor constituent of the liquid solution. Additionally, in this condition, the activity of the solved hydrogen can be equalized, with good approximation, to its molar concentration (C_H). Therefore, equation (40) can be simplified as:

$$K_{SOL} = \frac{C_H^2}{P_{H_2}} \tag{41}$$

which permits to calculate the concentration of solved hydrogen as:

$$C_H = (K_{SOL} \cdot P_{H_2})^{1/2} = K_S \cdot P_{H_2}^{1/2} \tag{42}$$

Equation (42) indicates that the hydrogen concentration in the liquid alloy is given by the product of the square root of the hydrogen pressure in the gas phase and of the constant K_S; K_S, defined as the Sieverts' constant, is hence given by:

$$K_S = C_H \cdot P_{H_2}^{-1/2} \tag{43}$$

and its unit of measurement corresponds to a concentration divided by the square root of a pressure. More details about the correct unit of measurements will be given in section 4.5.1.3.

4.5.1.2. Rough theoretical prevision of the hydrogen solubility in Pb-Li. The knowledge of the Hydrogen solubility (hence of the corresponding Sieverts' constant) in the eutectic liquid Pb-Li is of paramount importance in the application of this liquid alloy as breeding blanket, inasmuch the ^3H produced in the blanket by the impinging neutron flux needs to be extracted from the blanket itself in order to be recycled to the plasma fusion reaction. It is clear that, the lower is the solubility of ^3H, the larger will be its fraction moving to the gas phase and easier it will be to readdress this isotope to the core of the reactor; additionally, the ^3H inventory inside the blanket will result smaller, reducing the associated safety issues.

Since unfortunately, as will be detailed in section 4.5.2, the experimental values of the Hydrogen Sieverts' constant reported so far in literature are largely dispersed (several orders of magnitude!), we present here a preliminary, rough theoretical estimation of its expected value. Let's consider at first at the Hydrogen solubility values in pure liquid Lithium and in pure liquid Lead. Without searching for too accurate values (also for pure metals a small degree of uncertainty is present), it suffices to observe that there is a large difference between the solubility in Lead and in Lithium. Lead is characterized in fact by one of the lowest hydrogen solubility among the known metals (the dissolution process appears to be even endothermic), with the most reliable value reported for the Sieverts' constant equal to $\sim 6{\cdot}10^{-9}$ $Pa^{-1/2}$ at 600 °C [81] (and with a small dependence on temperature, though scarcely investigated). Quite the opposite, Lithium has one of the maximum capability to solubilize hydrogen among known metals, with a Sieverts' constant decreasing with temperature from ~1 $Pa^{-1/2}$ at the eutectic melting temperature to $\sim 6{\cdot}10^{-4}$ $Pa^{-1/2}$ at 1000 °C. This means that, up to this temperature, Hydrogen solubility in liquid Lithium results at least 5 orders of magnitude higher than in liquid Lead.

From this evidence, Larsen [81] concluded that the solubilisation of Hydrogen in Lead-Lithium solutions was due only to the presence of Lithium, while any interaction between Hydrogen and Lead had to be neglected. In this regard, we know that Lithium-Lead solutions are certainly not ideal, and that a kind of ionic interaction exists between the heteroatoms, leading to the partial formation of aggregates. This means that Lithium atoms in Pb-Li solutions are less available to solve and interact with Hydrogen than in pure Lithium: the degree to which Lithium is available and reactive in the solution is actually expressed by its chemical activity, which is no more unitary, as in the case of pure Lithium. Fig. 17 shows the values of Lithium activity vs temperature in a $Li_{17}Pb_{83}$ liquid solution, as calculated from previous experiments based on both electrochemical [19,82,83] and vapour pressure techniques [84]. In the figure, a substantial agreement between the results of the different authors can be noted; it is also evident that Lithium activity results largely smaller than its atomic fraction, going from $\sim 10^{-4}$ at 500 °C to $\sim 1.5{\cdot}10^{-3}$ at 800 °C. The increase of the activity with temperature makes sense, since at higher temperature the Lead-Lithium interaction is weakened and Lithium atoms become freer.

Larsen [81] modelled the dissolution of Hydrogen in liquid Lithium and similarly in Lead-Lithium solutions by assuming that in the liquid phase each Hydrogen atom is solved, on the average, by 1 Lithium atom, as a formal Li-H association existed. The generic equilibrium (39) becomes hence:

$$H_2(g) + 2\,Li \rightleftharpoons 2\,Li\text{-}H\,(sol) \tag{44}$$

and the corresponding constants in pure Li and in Pb-Li are expressed hence as:

$$K_{SOL(Li)} = \frac{a^2_{Li\text{-}H\ (Li)}}{P_{H_2}\, a^2_{Li}} = \frac{C^2_{Li\text{-}H\ (Li)}}{P_{H_2}} = K^2_{s\ (Li)} \tag{45a}$$

in the case of pure Li, and

$$K_{SOL(Pb\text{-}Li)} = \frac{a^2_{Li\text{-}H\ (Pb\text{-}Li)}}{P_{H_2}\, a^2_{Li}} = \frac{C^2_{Li\text{-}H\ (Pb\text{-}Li)}}{P_{H_2}\, a^2_{Li}} = \frac{K^2_{s\ (Pb\text{-}Li)}}{a^2_{Li}} \tag{45b}$$

in the case of the Pb-Li eutectic solution.

The 2 K_{SOL} constants must be numerically equal, since, in the assumption of no active role played by the Lead, they give the equilibrium ratio of the same quantities; this means that:

$$K_{s(Pb\text{-}Li)} = K_{s(Li)} \cdot a_{Li} \tag{46}$$

According to the relation (46), it is therefore possible to obtain the value of the Sieverts' constant in Pb-Li by multiplying the known value of Sieverts' constant in pure Lithium by the known Lithium activity in Pb-Li solution. Working this way Larsen got for $K_{s(Pb\text{-}Li)}$ a value almost constant with temperature in the range 500°C–767 °C, slightly decreasing from $\sim 1.5{\cdot}10^{-6}$ $Pa^{-1/2}$ (at 500 °C) to $\sim 1.2{\cdot}10^{-6}$ $Pa^{-1/2}$ (at 767 °C). This small dependence on temperature occurs because, from one side, the Sieverts' constant in pure Lithium decreases with temperature, while, from the other side, the activity of Lithium in the eutectic Pb-Li increases with temperature (as shown in Fig. 17): the 2 effects tend to compensate almost cancelling each other.

Later, Schumacher [85] corrected the model adopted by Larsen, since, based on the previous analysis of Frohberg [86], he underlined that the presence of Pb would affect instead, to some extent, the thermodynamics of the solubilisation process. Particularly, he highlighted that the state of the Hydrogen atoms in Pb-Li solutions is actually

Table 9
Density and conversion coefficient at selected temperature values. Sieverts' constant expressed as [mol m^{-3} $Pa^{-1/2}$] must be divided by the corresponding coefficient to be converted to [$Pa^{-1/2}$].

T [K]	508	600	700	800	900	997
PbLi density [Kg m^{-3}]	9957	9844	9722	9599	9476	9356
Conv. Factor [mol mol^{-3}]	56654	56010	55311	54612	53913	53234

different with respect to those in pure Lithium, because in the former situation the partial excess entropy of the dissolved Hydrogen results smaller. In his description, the presence of Lead alters the Hydrogen random distribution inside the solution and creates an energy barrier to the translation motion of Hydrogen atoms, which, similarly to Lead ones, acquire a partial negative electric charge from the surrounding Lithium atoms. A reduced excess entropy makes the dissolution less favoured and translates into a smaller value of the Sieverts' constant: according to Schumacher, the real hydrogen solubility in the eutectic Pb-Li alloy should result about 1 order of magnitude smaller than the one proposed by Larsen.

Summarizing this section, the theoretical investigations reported in literature for the Hydrogen solubility in the eutectic (or close to eutectic) Pb-Li solutions fix the value of the corresponding Sieverts' constant around 10^{-6}-10^{-7} $Pa^{-1/2}$ and indicate a rather small dependence on temperature. This preliminary, theoretical result, though still qualitative, can anyway constitute an additional parameter to assess the soundness of the experimental results later reported.

4.5.1.3. The unit of measurement of the Sieverts' constant. As stated in the previous section, the unit of measurement of the Sieverts' constant corresponds to a concentration divided by the square root of a pressure. By looking at the many values reported in literature for this constant, it is common anyway to find different ways to express it, because sometimes pressure is expressed as [*Pa*], sometimes as [*torr*], sometimes as [*bar*] … and similarly the concentration is expressed both as [*mol* m^{-3}] and as *molar fraction* (dimensionless number or [*appm*]). To complicate

Table 10
List (in chronological order) of significant Sieverts' constant values reported so far in literature [90,94].

Year	First Author	Employed technique	Li mol fraction	Investigated conditions	K_S value(s)
1985	Katsuta [89]	**Desorption**	~ 0.17	T = 573-708 K P = 10-100 kPa	$1.1 \cdot 10^{-6}$ $Pa^{-1/2}$ (constant in that range of T)
1988	Fauvet [90]	**Desorption**	~ 0.168	T = 723 K P = 2, 10 kPa	$2.7 \cdot 10^{-8}$ $Pa^{-1/2}$
1991	Feurstein [91]	**Permeation**	~ 0.168	573-883 K P = 5 Pa-100 kPa	$1.96 \cdot 10^{-7} \cdot exp\ (-3622/T) Pa^{-1/2}$ (573 K ⇒ $3.53 \cdot 10^{-10}$ $Pa^{-1/2}$) (883K ⇒ $3.25 \cdot 10^{-9}$ $Pa^{-1/2}$)
1991	Reiter [88]	**Desorption**	~ 0.166	T = 508-700 K P = 1-100 kPa	$2.4 \cdot 10^{-8} \cdot exp\ (-162.5/T) Pa^{-1/2}$ (508 K ⇒ $1.74 \cdot 10^{-8}$ $Pa^{-1/2}$) (700 K ⇒ $1.90 \cdot 10^{-8}$ $Pa^{-1/2}$)
2006	Aiello [92]	**Absorption**	0.158	T = 623-903 K P = 2.06-8.38 kPa	$4.3 \cdot 10^{-6} \cdot exp\ (-1546/T)$ $Pa^{-1/2}$ (623 K ⇒ $3.6 \cdot 10^{-7}$ $Pa^{-1/2}$) (903 K ⇒ $7.8 \cdot 10^{-7}$ $Pa^{-1/2}$)
2011	Edao [93]	**Permeation**	~ 0.17	T = 573-973 K P = 1-100 kPa	From ~1 to $3 \cdot 10^{-7}$ $Pa^{-1/2}$ (slight increase with T, but no sound correlation)
2012	Okitsu [94]	**Permeation**	~ 0.17	T = 773-973 K (P not specified)	~ $10^{-4} \cdot exp\ (-6560/T) Pa^{-1/2}$ (773 K ⇒ $2.1 \cdot 10^{-8}$ $Pa^{-1/2}$) (973 K ⇒ $1.2 \cdot 10^{-7}$ $Pa^{-1/2}$)
2013	Kumar [95]	**Absorption**	~ 0.15	T = 573-773 K P = 79-105 kPa	In the range: 2.35 - $4.51 \cdot 10^{-7}$ $Pa^{-1/2}$ (not monotonic trend: K_S max value at ~ 673 K)
2015	Alberro [96]	**Both Absorption and Desorption**	~ 0.17	T = 523-922 K P = $1\text{-}10^5$ Pa	$1.54 \cdot 10^{-7} \cdot exp\ (-108.3/T)$ $Pa^{1/2}$ (523 K ⇒ $1.25 \cdot 10^{-7}$ $Pa^{-1/2}$) (922 K ⇒ $1.37 \cdot 10^{-7}$ $Pa^{-1/2}$)
2021	Candido [97]	**Both Absorption and Desorption**	0.157	T = 573 K P = 2.5 KPa	Absorption: $4.16 \cdot 10^{-7}$ $Pa^{-1/2}$ Desorption: $3.18 \cdot 10^{-7}$ $Pa^{-1/2}$

the comparison of the different values, some of the oldest works in literature even report the Sieverts' constant as the reverse quantity of the currently accepted one (relation (41) of this report), i.e. as the square root of the gas pressure divided by the Hydrogen concentration in the liquid solution, and this of course is accompanied by a reverse unit of measurement and by a complication in visualizing the current trend of the constant with the temperature.

To avoid confusion, in this paper the employed unit constant will be only [$Pa^{-1/2}$]. It must be noted that to convert from [$mol\,m^{-3}\,Pa^{-1/2}$] to [$Pa^{-1/2}$] there is not fixed multiplicative coefficient. This is because the molar concentration [$mol\ m^{-3}$] depends of course, not only on the amount of Hydrogen solubilized in the Pb-Li solution, but also on the volume of the solution, which varies with temperature. Therefore, the knowledge of the solution volume variation with temperature (or, which is the same, of its density) is necessary to make the correct conversion at each specific temperature.

In order to convert [$mol{\cdot}m^{-3}$] to *molar fraction* (neglecting the mass effect of the few solved hydrogen atoms and the possible evaporation of the solvent atoms at the higher temperatures) it is necessary to divide the former unit by the solvent density (ρ) and to multiply it by its molar mass (0.17576 kg mol^{-1} for the exact $Li_{15.7}Pb_{84.3}$ composition). Previously, in this document, we selected equation (20) as the most accurate for the evaluation of the eutectic density variation with temperature:

$$\rho\ [\mathrm{Kg\ m^{-3}}] = (10581.8 \pm 35.5) - (1.229 \pm 0.027) \cdot T \text{ (valid for } 508 \leq T \leq 997\ \mathrm{K}) \quad (20)$$

By employing the above equation, it is possible to obtain the correct conversion coefficients at each temperature. Some of them are reported, as examples, in Table 9.

4.5.1.4. Differences in the solubilities of the hydrogen isotopes. For the application of Pb-Li as breeding blanket, what is actually important is the knowledge of the ^3H solubility inside the metallic liquid alloy. Anyway, disposing of and handling ^3H in a common lab setup is quite complicated, because of its low availability (and consequently high cost) and the relevant safety issues it poses. Therefore, until now, the investigation of hydrogen solubility in Pb-Li has been based on the study of ^1H or sometimes ^2H behaviour, while ^3H has been employed in a very few cases, even if in a close future new facilities are expected to focus their experimentation on the heaviest isotope [87].

Some small difference would actually exist in the different isotopes solubilities and in the related Sieverts' constants, yet it must be highlighted that this isotopic effect surely constitutes a very small contribution with respect to the large discrepancies (orders of magnitude) reported until now in the measured constant's values. From a theoretical point of view, even if an exact description of the system would require the very deep knowledge of the Pb-Li-H system, it is possible to qualitatively expect that the solubility would decrease a bit with the hydrogen nucleus mass, considering that in the gas phase the stability of the diatomic hydrogen molecule increases with the mass of its nuclei, while a similar isotopic effect in the liquid Pb-Li phase results less pronounced. In this regard, the experimental comparison made by Reiter [88] reported for ^2H a Sieverts' constant value ~ 3.5 % smaller than for ^1H in the same conditions.

In view of this trivial difference, we will list and consider all the experimental Sieverts' constant values in literature, regardless of the type of Hydrogen isotope they were describing: other aspects, certainly not the isotopic effect, must be responsible for the large uncertainty still affecting the value of this constant.

4.5.2. Sieverts' constant data from literature

4.5.2.1. General overview of the experimental works. A list of the most significant experimental works that, during the last decades, determined Hydrogen Sieverts' constant in eutectic (or near eutectic) Pb-Li liquid solutions is reported in Table 10. Each of them is synthetically described by the date (in chronological order), the first author name, the employed measurement technique, the investigated Pb-Li composition (Li mol fraction), the operative temperature and pressure values and, of course, the achieved K_S value(s) and/or the trend of K_S with temperature. All the K_S values have been expressed as [$Pa^{-1/2}$], implying that the concentration of solved Hydrogen is in term of molar fraction; to get the homogeneity of the units of measurement, in some cases it has been necessary to perform a conversion of the concentration and/or the pressure original units, according to the observations made in section 4.5.1.3. It is immediate to note the large discrepancy in the achieved values of K_S, which spread over a range of 4 order of magnitudes, from a minimum of ~10^{-10} to a maximum of ~10^{-6} $Pa^{-1/2}$.

The possible causes of so big differences may be.

a. The differences in the real compositions of the investigated samples. This doesn't mean only the formal Li molar fraction declared by the author (and indicated in the 4th column of Table 10), but includes also the preparation procedure of the eutectic alloy starting from the 2 metals and the accuracy (of the author) in verifying it. It is true that the differences in Li concentrations are small (a few %), nonetheless we know that, due to the quite dissimilar solubility of Hydrogen in Lead and Lithium, they can produce on the Sieverts' constant a larger effect than on any other property previously described in this paper. Additionally, the purity of the sample, i.e. the presence and the relative amounts of elements other than Li e Pb, may add a not negligible effect on the Hydrogen solubility: the presence of Oxygen, for instance, would increase the Hydrogen uptake.
b. The differences in the experimental setup and technique employed by the authors to measure it. In this regard, the techniques can be divided into 3 main categories: absorption, desorption and permeation. In the 3rd of column of Table 10, for an easier visualization, each different technique has been written with a different colour.
c. Finally, it must be also highlighted that every experiments aimed at determining the solubility of Hydrogen in a condensed phase sample (and not only in this specific case of a Pb-Li sample) requires always a big care in properly considering also the possible Hydrogen absorption/desorption on/from the materials the apparatus is made of, as well as the possible leaks of Hydrogen outside, and that pressure and temperature values must be precisely acquired. For this reason, employed equipment materials must be characterized by a minimal hydrogen absorption and permeation; additionally, a 'blank calibration' of the apparatus must be preliminarily conducted in order to evaluate the response of the measuring system in absence of the sample. All these aspects, if not properly managed, could generate a difference in the Sieverts' constant results as well. Unfortunately, often the numerical details of these preparative phases are not reported in the paper, so it is not possible to verify if correct numbers have been employed by the author.

Despite the big differences in the shown values of K_S are certainly discouraging, it is possible anyway to reduce to some extent the uncertainty around this constant, by analysing in details the 3 different, employed measurement techniques: this is discussed in the next section.

4.5.2.2. Differences in the employed measurement techniques. The quantification of Hydrogen concentration in a Pb-Li liquid solution would result conceptually easy if an electrochemical sensor, specifically selective only to Hydrogen element or ion, would exist. Unfortunately, such a sensor is not available yet, even if several research activities are today being conducted with the goal of developing and characterizing a device like this. Therefore, up to now, the quantification of Hydrogen concentration in the eutectic solution has been achieved only indirectly, in all the three main techniques already mentioned (absorption, desorption, permeation).

For what concerns the absorption and the desorption techniques, both of them are able to quantify the amount of Hydrogen solved in the eutectic liquid Pb-Li by the difference between a starting and a final gas phase situation, i.e. by the variation, during the experiment, of the H_2 pressure in the gas phase (which decreases in the absorption experiment, while increases in the desorption one): for the calculation it is of course necessary to know also both the gas phase volume and its temperature. To get the Sieverts' constant value, assumptions are needed both in the absorption and the desorption techniques, but those which underlie the desorption case are certainly less solid, as below detailed.

In the absorption technique, the test cell containing the Pb-Li sample is preliminarily evacuated in order to remove volatile impurities from the sample, including preabsorbed Hydrogen: at the end of this step, Hydrogen is assumed to be 0 in the gas phase and, consequently, in the liquid solution phase. This is the first assumption, which is anyway reasonable, since the possible residues of Hydrogen are surely minimal with respect to the amount later introduced inside the system. Then the test cell is suddenly (in few seconds) filled with Hydrogen up to a known, measured Hydrogen pressure, which represents the starting situation of the experiment: henceforward, due to the solubilisation in Pb-Li, H_2 pressure will go decreasing until a final constant value is achieved (end of the experiment). **The main assumption in this kind of procedure is hence that during the few seconds of pressurization with Hydrogen, no Hydrogen dissolution inside the liquid solution takes place**, so that the maximum detected gas pressure corresponds to the total amount of introduced Hydrogen. This way, indicating the starting and the final H_2 pressure in the gas phase respectively as P_0 and P_{end}, from the mass conservation in the two-phases system it is possible to get the value of K_S as:

$$K_S \left[\text{mol m}^{-3}\ \text{Pa}^{-0.5}\right] = \frac{2}{RT_{gas}} \frac{V_{gas}}{V_{Pb\text{-}Li}} \frac{P_0 - P_{end}}{P_{end}^{1/2}} \tag{47}$$

The desorption experiments requires instead a starting value of Hydrogen concentration in Pb-Li different from 0, being instead H_2 pressure in the gas phase equal to 0. In order to indirectly know the concentration in Pb-Li, it is necessary at first to perform an Hydrogen absorption step, at the end of which the equilibrium condition between residual Hydrogen in the gas phase and in the Pb-Li solution is established. Indicating the value of the corresponding Hydrogen pressure as P_0, its corresponding concentration in Pb-Li, C_o, will hence result:

$$C_0 = K_S \cdot P_0^{1/2} \tag{48}$$

which, for the moment is unknown, but is related through K_S to the known (measured) P_0 value.

At this point, the test cell is suddenly evacuated (high/ultra-high vacuum) to reduce the value of Hydrogen pressure very close to 0; this corresponds to the start of the experiment. **The assumption here is that the evacuation procedure may result so fast not to change the Hydrogen concentration in Pb-Li solution**, as if, during the evacuation phase, no mass transfer between the 2 phases occurred. Then, once the gas pressure has fallen down to 0, the system is isolated from the pumping system and Hydrogen starts desorbing from the liquid Pb-Li: Hydrogen pressure increases, until a new equilibrium condition is achieved, defined by a constant pressure value, P_{end}, and by a corresponding concentration C_{end} in solution, given by:

$$C_{end} = K_S \cdot P_{end}^{1/2} \tag{49}$$

Considering the hydrogen mass conservation in the two-phases system, it is possible to calculate the value of K_S this time as:

$$K_S \left[\text{mol m}^{-3}\ \text{Pa}^{-0.5}\right] = \frac{2}{RT_{gas}} \frac{V_{gas}}{V_{Pb\text{-}Li}} \frac{P_{end}}{P_0^{1/2} - P_{end}^{1/2}} \tag{50}$$

If, from the calculation point of view, this measurement technique is as easy as the absorption one, anyway the aforementioned assumption about the fast system evacuation seems not too good: it would be exact if the evacuation time was 0, but, since pressure goes to 0 asymptotically and the speed of evacuation depends on the real power and features of the pumping system, evacuation time results not negligible (it is not always indicated in literature, but it is of the order of several tens of seconds; Fauvet [91], for instance, reported 35–50 s in its experiments). During this time, some Hydrogen could actually be pumped away from the first layers of Pb-Li and it would not be considered in the following mass balance, affecting the correct numerical evaluation of the Sieverts' constant. More precisely, the desorption of Hydrogen already during the evacuation step would lead to a P_{end} value minor than the theoretical one, hence, according to equation (50), to a smaller Sieverts' constant.

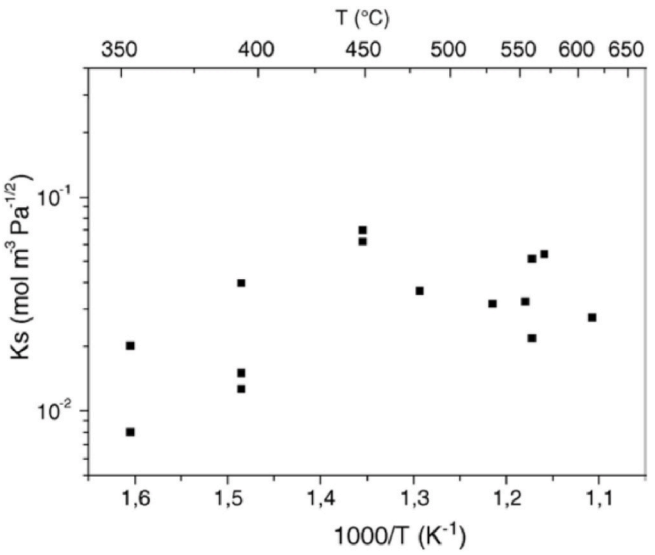

Fig. 18. K_S values achieved in the experiments by Aiello [92]*
* Reprinted from Fusion Engineering and Design, 81, A.Aiello et al., Determination of hydrogen solubility in lead lithium using sole device, 639–644, Copyright (2006), with permission from Elsevier.

Moreover, another issue of the desorption technique is that it generally requires vacuum conditions more pronounced than the absorption one. In these vacuum ($\ll$ 1 Pa) and temperature (>500K) conditions, metals volatility cannot be ignored at all; in particular, being Li more volatile than Lead [98], it would evaporate preferentially from the solution (in terms of numbers of atoms), so its molar fraction here would be reduced with the respect to the original one. As stated in section 4.5.1.2, a smaller Li concentration would translate into a smaller Sieverts' constant.

For all these reasons, we expect that desorption experiments could underestimate the Hydrogen solubility in eutectic Pb-Li; not by chance, Sieverts' constant determined by the desorption experiments, especially the oldest one, generally result significantly smaller than those by the absorption experiments (see Table 10). Only Katsuta [89] determined a value in decent agreement with those by absorption, but it must be noted that his procedure, not exhaustively described in his paper, was anyway a bit different from the usual desorption ones, because it entailed also an additional intermediate step, consisting in quenching the sample to room temperature (hence to solid state) after the equilibration phase and before the start of the desorption step.

Regarding the Sieverts' constant measurement through the **permeation technique**, there is not a good intrinsic agreement among the different values reported by the many authors (from 10^{-10} to 10^{-7}), even if, on the whole, it can be said they are generally smaller than those achieved through the absorption technique (see Table 10). Without entering the complex details of each specific work, the general feature of the permeation technique is that, differently from the other methods previously described, the Sieverts' constant here is calculated not from

Table 11
K_S values reported by Kumar at different temperatures [95].

T [°C]	300	350	400	500
K_S [$Pa^{-1/2}$]	$2.35 \cdot 10^{-7}$	$4.43 \cdot 10^{-7}$	$4.49 \cdot 10^{-7}$	$4.41 \cdot 10^{-7}$

the ratio of quantities in equilibrium condition at the end of the experiment, but from 'transient curves', i.e. as one the fitting parameters of an ensemble of kinetic equations. The permeation process is constituted by a series of sequential steps (Hydrogen gas entering the measuring cell from the bottom; Hydrogen absorption on the bottom surface of the plate supporting the liquid Pb-Li, generally made of α-Fe; diffusion through the α-Fe plate; mass equilibrium at the α-Fe/Pb-Li interface; hydrogen diffusion through the Pb-Li sample layer; H_2 desorption from the top of the Pb-Li sample to the above volume; purging out, from the top, of the desorbed H_2), therefore it is clear that the large number of equations and assumptions/boundary conditions that underlie them can negatively affect, in terms of accuracy of the results, the constant determination. Also, it must be underlined that, in a dynamic experiment, thermodynamic equilibrium conditions are not established, while a stationary state is achieved (corresponding to the equality of the rates of the many steps) and this can sometimes lead to a wrong description of the system.

Being therefore the absorption experiments those affected by the smaller level of approximation in the system description, they are supposed to lead to the more accurate evaluation of the hydrogen solubility. Additionally, most of the absorption experiments listed in Table 10 investigated Pb-Li alloy samples with a composition equal or very close to the real eutectic one, while reported desorption/permeation experiments are related to a higher Lithium concentration (16.8–17 at.%). Therefore, the outcome of the absorption experiments is considered the most trustable one and will be detailed more in section 4.5.2.3.

A final general consideration regarding the absolute values of the Sieverts' constant: even considering the maximum values reported in Tables 10 and i.e. approximately 10^{-6} $Pa^{-1/2}$ (Katsuta [89]), and calculating the corresponding Hydrogen concentration in equilibrium even with a high gas pressure (of the order of 10^5 Pa), we get the value of ~300 appm, which is lower than the minimum one required to produce LiH precipitation in pure liquid Lithium at 200 °C, i.e. 437 appm [80]. Since we know that Lithium activity in eutectic Pb-Li is quite smaller than in the pure alkali metal, we can be even more sure that no solid phase forms inside the system and that hydrogen only moves between a gas and a liquid phase.

4.5.2.3. Some considerations about the values of K_S from specific absorption experiments. In 2006 Aiello [93] employed the SOLE device to perform, through the absorption technique, the K_S measurement of a Pb-Li sample characterized, for the first time, by the correct eutectic composition ($x_{Li} = 0.157$). The SOLE device was constituted by the solubilisation chamber and by the liquid solution charging and discharging system; the internal surface of the apparatus, made of stainless steels, was covered with a layer of Tungsten (W) deposited through the Plasma Vapour Deposition (PVD) process, in view of the very low solubility and permeability of Hydrogen in this transition metal. The level of contaminants in the Pb-Li sample was evaluated to be lower than 0.1 wt%.

Several measurements were performed, changing the starting H_2 pressure (in the range 2.06–8.38 kPa) and the Pb-Li temperature (in the range of 623–903K); the totality of the K_S values so achieved [mol m^{-3} $Pa^{-1/2}$] is graphically shown in Fig. 18.

Considering, for each temperature, the average of all the corresponding K_S values, the author inferred the correlation, which, after converting the unit of measurement, becomes:

$$K_S\ [Pa^{-1/2}] = 4.3 \cdot 10^{-6} \cdot \exp(-1546/T) \quad (51)$$

Actually, the experimental points seems rather scattered with respect to the fitting curve defined by this equation: it would also seem that there is no a sure monotonic trend with temperature, but that the maximum K_S value was located around an intermediate temperature. So, we keep as good from this experimentation only the range of the K_S values (~2–10 · 10^{-7} $Pa^{-1/2}$) and its rather small variation with temperature.

This range of values is in good agreement with the one indicated by Kumar [95], who investigated Pb-Li samples with a (verified) Li molar fraction of ~0.15 and employing an apparatus made of quartz (low permeability to Hydrogen), both its reaction chamber and its sample holder. Here again, it seems that the K_S value decreases (or at least increases more) with temperature after reaching a maximum at around 400 °C (see Table 11): due to this not monotonic trend, the author didn't propose a K_S vs T correlation.

In 2015 Alberro [96] evaluated the Sieverts' constant employing both the absorption and the desorption techniques on the same Pb-Li sample; in his setup, the ultra-high vacuum (10^{-7} Pa) was obtained by means of two pumping units (comprising a turbomolecular and a two-stage rotary pump each), which allowed to reduce somehow the duration of the depressurization (pumping out) step. Differently from the previous experiments, after loading the gas inside the sample cell he didn't wait the establishing of a constant (minimal) H_2 pressure before starting the evacuation step: he modelled instead the pressure evolution during the loading step through the Fick's laws, i.e. with a kinetic equation depending on both the hydrogen solubility and its diffusivity in Pb-Li; these quantities were then obtained through a non linear least squares fitting routine (absorption measurement). Similarly, by fitting the kinetic equation describing the gas pressure evolution during the hydrogen release step, he got hydrogen solubility and diffusivity related to the desorption experiment.

The main outcome of Alberro work is that 'absorption' and 'desorption' Sieverts' constant values this time are very similar, and for this reason he didn't described them separately, but proposed a unique correlation holding for all of them, which, after converting the unit of measurement, becomes:

$$K_S\ [Pa^{-1/2}] = 1.54 \cdot 10^{-7} \cdot \exp(-108.3/T) \quad (52)$$

Here we can see the even more smaller dependence on temperature with respect to equation (51) and to Kumar values. In fact, according to equation (52), K_S would result almost constant, increasing from $1.25 \cdot 10^{-7}$ $Pa^{-1/2}$ to only $1.37 \cdot 10^{-7}$ $Pa^{-1/2}$ in the investigated range of temperatures (523–922 K).

Alberro values are on the whole slightly smaller than Aiello's and Kumar's ones. In this document, they are actually considered a bit less trustable then the 2 previous ones, because the sample was here investigated starting from a not equilibrium situation and the assumptions which underlie the kinetic modelization are not always fully convincing; mostly, the author himself reported that, due the exposition to the ultra-high vacuum conditions, the Pb-Li sample decreases its mass by a few % after the experiment execution. Taking into account that the volatility of Lithium is relatively greater than Lead one, the occurred evaporation would have increased the Lead content in the liquid alloy, decreasing therefore the Sieverts' constant value. This could justify the smaller values reported by Alberro; which, in any case, are characterized by the same order of magnitude of Aiello's and Kumar's.

Due to the discussed lack of trustable values, today the topic of Hydrogen Sieverts' constant in eutectic Pb-Li is still under investigation and new experiments are being conducted to improve the accuracy of the measurement. Within them, the device *HyPer-QuarCh II* must be mentioned [97,99]. This device features a crucible for the sample made of Tungsten and a test section realised in quartz; quartz is interfaced to metal through KF connections and an upper flange hosting 3 sleeves, with grooves which house nitrile rubber O-rings. The most relevant aspect of *HyPer-QuarCh II* are anyway the crucible heating system,

which is based on a 500W Infrared collar made of quartz with a gold shielding for the radiation collimation, and which results extremely efficient; and the short evacuation time (preliminary to the start of the desorption experiment), which is reduced to only 8s (and in future, with further improvements, could be reduced more), thanks to the employment of a *Pfeiffer ACP 15 dry roots* pump instead of a turbomolecular pump; the latter, requiring a smaller initial pressure gradient hence an additional backing pump to operate, on the whole needs more time to generate a stable vacuum condition.[5]

Up to now, only 1 temperature (573K) and 1 pressure (2.5 kPa) have been investigated with *HyPer-QuarCh II*. The interesting outcome of this first experimentation is that the Sieverts' constant measured through the absorption technique ($4.16{\cdot}10^{-7}$ $Pa^{-1/2}$) is quite similar to the one obtained through the desorption one ($3.18{\cdot}10^{-7}$ $Pa^{-1/2}$), witnessing that the Hydrogen loss from the Pb-Li sample during the long evacuation step surely was one of the most important reasons of the different results, obtained in the previous decades, between the 2 measurement techniques. Additionally, it must be noted that the values obtained through *HyPer-QuarCh II* are also similar to those by Aiello and Kumar.

HyPer-QuarCh II experimentation has just started, so additional temperature and pressure conditions are expected to be dealt with in close future papers. For the correct evaluation of the Sieverts' constant value, it should however be explained better which is the true value of the gas phase temperature to put in the calculation equations, since actually the *HyPer-QuarCh II* test cell is not isotherm, but characterized by a temperature decreases from the bottom (interface with the Pb-Li liquid alloy: it defines the temperature of the experiment) to the top (~348 K on the steel flange).

4.5.3. Range of trustable Sieverts' constant values

At the end of this wide section about the Hydrogen Sieverts' constant in eutectic Pb-Li, it isn't yet possible to indicate an exact, trustable correlation to calculate its value at a specific temperature. It has been anyway shown that measurements based on absorption techniques are affected by minor approximations in the calculation procedure than other techniques, therefore they are able to produce more accurate results; moreover, results through the absorption technique are also intrinsically closer each other.

From the reported experimental evidences, it's therefore at least possible.

- to attribute to K_S a value in the range of 2–4 $\cdot 10^{-7}$ $Pa^{-1/2}$ at the temperature of 573K;
- to highlight the small variation of K_S with temperature. The monotonic trend at the moment is not sure, anyway in no case the maximum value reached by K_S (for temperatures up to 903K) should exceed 10^{-6} $Pa^{-1/2}$.

The soundness of the values above indicated is also confirmed by the good agreement with the outcome of the theoretical estimations discussed in section 4.5.1.2. In this regards, it must be also noted that very smaller K_S values, of the order of 10^{-9} $Pa^{-1/2}$ or even 10^{-10} $Pa^{-1/2}$, like those coming from some old measurements based on desorption or permeation techniques, appear surely not reasonable, since they would suggest that the hydrogen solubility in Pb-Li is even smaller than in pure Lead.

In order to further reduce the uncertainty around the value of K_S and its variation with temperature, additional 'desorption' experimentation should be conducted in future, in which all the already considered aspects (testing and qualification of the chemical composition of the

[5] The first *HyPer-QuarCh II* configuration was actually based on a turbomolecular pump supported by a backing pump: with such a configuration, around 1 min was necessary to evacuate the test cell before the desorption step could start.

Table 12
Selected correlations and related features for the investigated thermophysical properties of liquid PbLi eutectic solutions.

Specific heat	
Unit of measurement:	$J\ g^{-1}\ K^{-1}$
Selected correlation:	$c_p = 0.2009 - 2.806 \cdot 10^{-5}\ T + 7.343 \cdot 10^{-9}\ T^2$
Range of validity:	508–1000 K
Description:	New correlation, obtained through the optimized, theoretical analysis of the experimental data reported by Schulz in 1986 [43].
Estimated accuracy and/ or precision:	The original data by Schulz were characterized by a relative std dev. Equal to 3 %. The selected correlation perfectly suits ($R^2 = 0.9997$) the recalculated experimental points.
Notes/conclusions:	Despite the experimental works that investigated the specific heat are actually a few, its value changes scarcely with temperature and composition, therefore there is no real need for a new, additional experimentation.
Density	
Unit of measurement:	$Kg\ m^{-3}$
Selected correlation:	$\rho = (10581.8 \pm 35.5) - (1.229 \pm 0.027)\ T$
Range of validity:	508–997 K
Description:	Correlation proposed by Khairulin in 2016 [55] and based on the investigation through the penetrating γ-rays technique.
Estimated accuracy and/ or precision:	The maximum uncertainty associated to the density value is calculated as ~0.67 % in relative terms.
Notes/conclusions:	The proposed correlation is supported by a solid experimentation, is well described and is characterized by a low numerical uncertainty, therefore there is no real need for a new, additional experimentation.
Volumetric thermal expansion coefficient	
Unit of measurement:	K^{-1}
Selected correlation:	$\beta = \frac{1}{8610 - T}$
Range of validity:	508–997 K
Description:	Correlation obtained through the simple mathematical transformation of the correlation selected for the density.
Estimated accuracy and/ or precision:	The maximum uncertainty associated to the density value is calculated as ~2.3 % in relative terms.
Notes/conclusions:	The soundness of this correlation is the same of the correlation for density, therefore there is no real need for a new, additional experimentation.
Thermal conductivity	
Unit of measurement:	$W\ m^{-1}\ K^{-1}$
Selected correlation:	$\lambda = 0.71 + 0.0291\ T - 1.064 \cdot 10^{-5}\ T^2$
Range of validity:	508–1273 K
Description:	Correlation proposed by Agazhanov in 2020 [61] and based on the investigation through the laser flash method.
Estimated accuracy and/ or precision:	The relative error estimated and declared by Agazhanov is in the range 4–6% (it increases at higher temperature).
Notes/conclusions:	It is not easy to experimentally measure the thermal conductivity, because the experiment must be conducted in dynamic conditions and heat losses to the environment are hard to accurately estimate. In view of this, the accuracy of the proposed correlation is considered satisfying. Moreover the soundness of the proposed correlation is strengthened by the perfect internal coherence with the correlation selected for the electrical resistivity, according to the resulting Lorenz number.
Thermal diffusivity	
Unit of measurement:	$mm^2\ s^{-1}$
Selected correlation:	$\alpha = 0.208 + 0.0160\ T - 4.405 \cdot 10^{-6}\ T^2$
Range of validity:	508–997 K
Description:	New correlation, analytically obtained from the above selected correlations for the Specific Heat, the Density and the Thermal conductivity.
Estimated accuracy and/ or precision:	The relative uncertainty is estimated as ≤ 7 %

(*continued on next page*)

Table 12 (*continued*)

Notes/conclusions:	This correlation follows straight from the previously reported ones and it is considered as trustable as them. If the best thermal conductivity correlation will be updated in future by the outcome of new experimentations, the correlation for the thermal diffusivity should be updated accordingly, keeping the same ones for Specific Heat and Density, which result satisfactorily accurate.
Electrical resistivity	
Unit of measurement:	μΩ cm
Selected correlation:	$\rho_{el} = 101.28–6.380 \cdot 10^{-3}\ T + 4.211 \cdot 10^{-5}\ T^2$
Range of validity:	600–800 K
Description:	New correlation, analytically obtained by adapting the Hubberstey experimental data [71] to the Lithium molar fraction exactly equal to 0.157.
Estimated accuracy and/ or precision:	It is not possible to associate to the above equation an intrinsic accuracy, because it follows from the original experimentation made by Hubberstey, who only declared the maximum admitted temperature uncertainty (±1K), but didn't evaluate all the possible sources of errors and of their propagation.
Notes/conclusions:	A direct measurement of the real eutectic sample should be executed in future, to confirm the correlation here proposed and to evaluate its trustability; the temperature range of validity should be extended as well. In any case, it worth's noting that this correlation assures a perfect internal coherence with the correlation selected for the thermal conductivity, according to the resulting Lorenz number.
Sieverts' constant	
Unit of measurement:	$Pa^{-1/2}$
Selected correlation:	No specific correlation selected for K_S. It is possible for moment to define only its order of magnitude: $K_S \sim 2–4 \cdot 10^{-7}$ at 573K; $K_S \leq 10^{-6}$ in the temperature range up to 903K
Range of validity:	573–903 K (only for the order of magnitude)
Description:	The order of magnitude of K_S is extracted from the data reported by [92,95,97]
Estimated accuracy and/ or precision:	In lack of a specific correlation, it's not possible to estimate it.
Notes/conclusions:	The Sieverts' constant is the only thermophysical property of this document for which a unique, trustable correlation cannot be proposed yet. Additional experiments are hence needed to overcome this issue. Many working group are therefore presently keeping investigating it, employing more and more accurate setups and calculation procedures.

investigated Pb-Li eutectic sample; minimization of the sample contamination during its handling; 'blank' correction; determination of the operative parameters – temperatures, pressures, volumes) should be implemented more and more accurately. Additionally, it could be also useful to conceive and conduct an in-depth experiment, based on the execution of several, sequential steps of Hydrogen adsorption by the same sample and at the same temperature, i.e. according to the scheme.

a. Evacuation of the test vessel containing the liquid eutectic solution;
b. First introduction of a measured amount of gaseous Hydrogen in the test vessel;
c. Adsorption of Hydrogen by the liquid solution, gas pressure decrease and stabilization;
d. Calculation of K_S from the stabilized pressure value;
e. Second introduction of a measured amount of gaseous Hydrogen in the test vessel (maybe the same amount of step b)
f. Replication of steps c-d-e, and so on, several times.

This way it could be possible to construct a plot of the adsorbed Hydrogen amounts against the introduced ones, and from its fitting to get additional info on the answer of the system. For example, if the intercept resulted $\neq 0$, it could indicate the existence of some external contribution (negative or positive) to the measured, stabilized Hydrogen pressure, and this could be due in turn to the desorption/adsorption of Hydrogen from/on the wall of the apparatus or to possible leaks; similarly, strange slopes could also indicate the inaccuracy in determing the parameters entering the calculation (P · V/T).

Mostly, the future, possible, availability of specific (electrochemical) sensors able to directly quantify the amount of Hydrogen solved in the Pb-Li solution would certainly permit to significantly improve the knowledge of the Pb-Li-H system.

5. Conclusions

The analysis of the numerous papers retrieved in literature has permitted to optimize the description of the Pb-Li systems. Starting from the phase diagrams and the many Pb_xLi_y compounds in solid phase, the attention has been then focused on the Pb-Li liquid solutions, particularly the one corresponding to the exact eutectic composition, i.e. $Pb_{84.3}Li_{15.7}$. The theoretical modelization of these liquid solutions has highlighted their non ideality, as indicated by the measured/calculated values of the Excess Mixing Entropy and Enthalpy, the Short Range Order parameter (SRO), the molar volume, the metals activity … It has been hence possible to conclude that a partial ionic interaction is established in solution between the hetero-metals, with the electronic density localized closer to the Lead atoms and the formations of poly-atomic clusters.

All this description has been useful to rationalize the behaviour of the Pb-Li solutions and to qualitatively evaluate the values of many of their chemical and physical properties, also allowing to foresee their variations with temperature and with small composition shifts. This has permitted to dispose of additional criteria to rank the soundness of the different correlations reported in literature and, when the exact eutectic composition hadn't been investigated yet, to calculate the best correlation for it from the experimental data related to the closest available composition.

The other criteria adopted to qualify each experimental work described in literature have been: the validity of the employed experimental setup and the working procedure; the intrinsic results goodness; the closeness of the experimental conditions to the Pb-Li working conditions in the blanket; the distance of the set of values collected in a specific experiment from the average of the whole data ensemble and the explanation given by the author to justify why his results differ from the others'. Adopting all the above criteria, it has been possible to find out the best correlations to describe the following thermophysical properties of the liquid eutectic solution: the specific heat, the density, the volumetric thermal expansion coefficient, the thermal conductivity, the thermal diffusivity, the electrical resistivity and the Sieverts' constant of Hydrogen. When a sufficiently trustable correlation couldn't be selected, a new, optimized one, has been proposed or, in case of the Sieverts' constant, a restricted range of trustable values has been at least indicated.

Each of the aforementioned properties has been detailed in the corresponding section of this document; anyway, to make easier and faster the consultation of the results, a synthetic outcome of the whole work is reported in Table 12.

CRediT authorship contribution statement

Paolo Favuzza: Writing – review & editing, Writing – original draft, Validation, Methodology, Investigation, Formal analysis, Data curation, Conceptualization.

Declaration of competing interest

The author declares that he has no known competing financial interests or personal relationship that could have appeared to influence the work reported in this paper.

Data availability

Data will be made available on request.

Acknowledgements

This work has been carried out within the framework of the EUROfusion Consortium, funded by the European Union via the Euratom Research and Training Programme (Grant Agreement No 101052200—EUROfusion). Views and opinions expressed are however those of the author only and do not necessarily reflect those of the European Union or the European Commission. Neither the European Union nor the European Commission can be held responsible for them.

References

[1] H. Okamoto, Li-Pb (Lithium-Lead), J. Phase Equil. 14–6 (1993) 770, https://doi.org/10.1007/BF02667896.
[2] P. Hubberstey, T. Sample, M.G. Baker, Is Pb-17Li really the eutectic alloy? A redetermination of the lead-rich section of the Pb-Li phase diagram ($0.0 < x_{Li}$(at%) < 22.1), J. Nucl. Mater. 191–194 (1992) 283–287, https://doi.org/10.1016/S0022-3115(09)80051-2.
[3] Grube G., Klaiber H., Z.Elektochem. 40 (1934), 745-754, https://doi.org/10.1002/bbpc.193400038.
[4] M.A. Rollier, E. Arreghini, La fase gamma della lega litio-piombo, $Li_{10}Pb_3$, Stechiometria e struttura, Z. Krist 101 (1939) 470–482, https://doi.org/10.1524/zkri.1939.101.1.470.
[5] A. Zalkin, W.J. Ramsey, Intermetallic compounds between lithium and lead. I. The structures of Li_3Pb and Li_7Pb_2, J. Phys. Chem. 60 (1956) 234–236, https://doi.org/10.1021/j150536a022.
[6] A. Zalkin, W.J. Ramsey, D.H. Templeton, Intermetallic compounds between lithium and lead. II. The crystal structure of Li_8Pb_3, J. Phys. Chem. 60 (1956) 1275–1277, https://doi.org/10.1021/j150543a030.
[7] A. Zalkin, W.J. Ramsey, Intermetallic compounds between lithium and lead. III. The β1-β transition in LiPb, J. Phys. Chem. 61 (1957) 1413–1415, https://doi.org/10.1021/j150556a034.
[8] A. Zalkin, W.J. Ramsey, Intermetallic compounds between lithium and lead. IV. The crystal structure of $Li_{22}Pb_5$, J. Phys. Chem. 62 (1958) 689–693, https://doi.org/10.1021/j150564a013.
[9] J.F. Smith, Z. Moser, Thermodynamic properties of binary lithium systems — a review, J. Nucl. Mater. 59 (1976) 158–174, https://doi.org/10.1016/0022-3115(76)90131-8.
[10] C. Zhou, C. Guo, C. Li, Z. Du, Thermodynamic optimization of the Li-Pb system aided by first-principles calculations, J. Nucl. Mater. 477 (2016) 95–101, https://doi.org/10.1016/j.jnucmat.2016.04.061.
[11] U. Jauch, V. Karcher, B. Schulz, G. Haase, Thermophysical properties in the system Li-Pb, KfK 4144 Report (1986). https://inis.iaea.org/search/search.aspx?orig_q=RN:18022137.
[12] H. Perlitz, E. Aruja, V. A redetermination of the crystal structure of lithium, Philos. Mag. A 7 (30) (1940) 55–63, https://doi.org/10.1080/14786444008520697.
[13] H.P. Klug, A.Redetermination of the lattice constant of lead, J. Am. Chem. Soc. 68 (8) (1946) 1493–1494, https://doi.org/10.1021/ja01212a032.
[14] C. Tyzack, V. Raynor, The lattice spacings of lead-rich substitutional solid solutions, Acta Crystallogr. 7 (1954) 505–510, https://doi.org/10.1107/S0365110X54001600.
[15] W. Geertsma, J. Dijkstra, W. van der Lugt, Electronic structure and charge-transfer-induced cluster formation in alkali-group-IV alloys, J. Phys. F Met. Phys. 14 (1984) 1833–1845, https://doi.org/10.1088/0305-4608/14/8/013.
[16] B. Predel, G. Oheme, Kalorimetrische Untersuchung flüssiger lithium-blei-Legierungen, Z. Metallkd 70 (1979) 450–453, https://doi.org/10.1515/ijmr-1979-700708.
[17] A.I. Demidov, A.G. Morachevsky, L.N. Gerasimenko, Russ. J. Electrochem. 9 (1973) 848–851.
[18] S.P. Yatsenko, E. Saltykova, Russ. J. Phys. Chem. 50 (1976) 2129–2130.
[19] M.L. Saboungi, J. Marr, M. Blander, Thermodynamic properties of a quasi-ionic alloy from electromotive force measurements: the Li–Pb system, J. Chem. Phys. 68 (1978) 1375–1384, https://doi.org/10.1063/1.435957.
[20] A. Neubert, Thermodynamic study of solid and liquid lithium + lead alloys using Knudsen-effusion mass spectrometry, J. Chem. Thermodyn. 11 (1979) 971–977, https://doi.org/10.1016/0021-9614(79)90046-6.
[21] M. Hoch, The solubility of hydrogen, deuterium and tritium in liquid lead-lithium alloys, J. Nucl. Mater. 120 (1984) 102–112, https://doi.org/10.1016/0022-3115(84)90177-6.
[22] C.H. Wu, The interaction of hydrogen isotopes with lithium-lead alloys, J. Nucl. Mater. 122 (1984) 941–945, https://doi.org/10.1016/0022-3115(84)90199-5.
[23] W. Gasior, Z. Moser, Thermodynamic study of liquid lithium-lead alloys using the EMF method, J. Nucl. Mater. 294 (2001) 77–83, https://doi.org/10.1016/S0022-3115(01)00440-8.
[24] H. Ruppersberg, H. Egger, Short-range order in liquid Li-Pb alloys, J. Chem. Phys. 63 (1975) 4095–4103, https://doi.org/10.1063/1.431179.
[25] H. Ruppersberg, H. Reiter, Chemical short-range order in liquid LiPb alloys, J. Phys. F. 12 (1982) 1311–1325, https://doi.org/10.1088/0305-4608/12/7/005.
[26] S. Mudry, I. Shtablavyi, Structure and electrophysical properties of liquid $Pb_{83}Mg_{17}$ and $Pb_{83}Li_{17}$ eutectics, J. Nucl. Mater. 376 (2008) 371–374, https://doi.org/10.1016/j.jnucmat.2008.02.011.
[27] A. Fraile, S. Cuesta-Lopez, A. Caro, D. Schwen, J.M. Perlado, Interatomic potential for the compound-forming Li-Pb liquid alloy, J. Nucl. Mater. 448 (2014) 103–108, https://doi.org/10.1016/j.jnucmat.2014.01.037.
[28] G. Kresse, J. Hafner, Ab initio molecular dynamics for liquid metal, Phys. Rev. B 47 (1993) 558–561, https://doi.org/10.1103/PhysRevB.47.558.
[29] G. Kresse, J. Hafner, Ab initio molecular-dynamics simulation of the liquid-metalamorphous- semiconductor transition in germanium, Phys. Rev. B 49 (1994) 14251–14269, https://doi.org/10.1103/PhysRevB.49.14251.
[30] G. Kresse, J. Furthmuller, Efficiency of ab-initio total energy calculations for metals and semiconductors using a plane-wave basis set, Comput. Mater. Sci. 6 (1996) 15–50, https://doi.org/10.1016/0927-0256(96)00008-0.
[31] G. Kresse, J. Furthmuller, Efficient iterative schemes for ab initio total-energy calculations using a plane-wave basis set, Phys. Rev. B 54 (1996) 11169–11186, https://doi.org/10.1103/PhysRevB.54.11169.
[32] S. Terlicka, A. Debski, W. Gasior, Thermodynamic properties of Li-Pb system, J. Mol. Liquids 249 (2018) 66–72, https://doi.org/10.1016/j.molliq.2017.11.013.
[33] W. Becker, G. Schwitzgebel, H. Ruppersberg, Thermodynamic investigations of liquid Li-Pb and Li-Ag-alloys — a Comparative study, Z. Metallkd. 72 (1981) 186–190, https://doi.org/10.1515/ijmr-1981-720306.
[34] J. Saar, H. Ruppersberg, Calculation of Cp(T) for liquid Li/Pb alloys from experimental ρ(T) and (δρ/δT)s data, J. Phys. F Met. Phys. 17 (1987) 305–314, https://doi.org/10.1088/0305-4608/17/2/003.
[35] B.E. Warren, X-Ray Diffraction, Addison Wesley, Reading, Mass, 1969.
[36] J.M. Cowley, An approximate theory of order in alloys, Phys. Rev. 77 (1950) 669–675, https://doi.org/10.1103/PhysRev.77.669.
[37] R.N. Singh, D.K. Pandev, S. Sinha, N.R. Mitra, P.L. Srivastava, Thermodynamic properties of molten LiMg alloy, Physica B 145 (1987) 358–364, https://doi.org/10.1016/0378-4363(87)90105-7.
[38] J.M. Cowley, Diffraction Physics, Elsevier, New York, 1975.
[39] F. Reiter, R. Rota, J. Camposilvan, Thermodynamic properties of $Li_{17}Pb_{83}$, Fusion technology, in: Proceedings of the 12. Symposium, Juelich, September 1982, pp. 13–17. https://inis.iaea.org/search/search.aspx?orig_q=RN:15068956.
[40] G. Kuhlborsch, F. Reiter, Physical properties and chemical reaction behaviour of $Li_{17}Pb_{83}$ related to its use as a fusion reactor blanket material, Nucl. Eng. Des. Fusion 1 (1984) 195–203, https://doi.org/10.1016/0167-899X(84)90040-5.
[41] IAEA, Thermophysical Properties of Materials for Nuclear Engineering: A Tutorial and Collection of Data, IAEA, Vienna, 2008. ISBN 978-92-0-106508-7, https://www.iaea.org/publications/7965/thermophysical-properties-of-materials-for-nuclear-engineering-a-tutorial-and-collection-of-data.
[42] M. Kondo, Y. Nakajima, M. Tsuji, T. Nozawa, Evaluation of thermal conductivity for liquid lead lithium alloys at various Li concentrations based on measurement and evaluation of density, thermal diffusivity and specific heat of alloys, Fusion Eng. Des. 109–111 (2016) 1345–1350, https://doi.org/10.1016/j.fusengdes.2015.12.029.
[43] B. Schulz, Thermophysical properties of the Li(17) Pb(83) alloy, Fusion Eng. Des. 14 (1991) 199–205, https://doi.org/10.1016/0920-3796(91)90002-8.
[44] E.A. Mogahed, G.L. Kulcinski, Bibliography of a Promising Trititum Breeding Material – $Pb_{83}Li_{17}$, Fusion Technology Institute, University of Wisconsin, 1995. UWFDM-994, https://fti.neep.wisc.edu/fti.neep.wisc.edu/pdf/fdm994.pdf.
[45] Malcom W., NIST-JANAF Thermochemical tables – lithium (Li), J. Phys. Chem. Ref. Data, Monograph 9, 1493-1527, https://www.google.com/url?sa=t&rct=j&q=&esrc=s&source=web&cd=&ved=2ahUKEwi9uamnwcL_AhXibvEDHTyhCbYQFnoECA0QAQ&url=https%3A%2F%2Fjanaf.nist.gov%2Fpdf%2FJANAF-FourthEd-1998-Lithium.pdf&usg=AOvVaw3nbqe1AYEId12YSnSpUBNi.
[46] Malcom W., NIST-JANAF thermochemical tables – lithium (Pb), J. Phys. Chem. Ref. Data, Monograph 9, 1835-1847, https://www.google.com/url?sa=t&rct=j&q=&esrc=s&source=web&cd=&ved=2ahUKEwiB5vrhwsL_AhWESPEDHZz_AzQQFnoECA0QAQ&url=https%3A%2F%2Fjanaf.nist.gov%2Fpdf%2FJANAF-FourthEd-1998-Lead.pdf&usg=AOvVaw0NHBQp7Z-g8sNOMTWqXxbr.
[47] F. Sommer, Experimental determination of the specific heats of liquid Li_7Pb_2 and LiPb alloys, Z. Phys. Chem. 156 (1988) 593–597, https://doi.org/10.1524/zpch.1988.156.Part_2.593.
[48] D. Martelli, A. Venturini, M. Utili, Literature review of lead-lithium thermophysical properties, Fusion Eng. Des. 138 (2019) 183–195, https://doi.org/10.1016/j.fusengdes.2018.11.028.
[49] A. Schneider, Heymer G. Stauffer, Über die Dichte flüssiger Metalle und Legierungen, Naturwissenschaften 41 (1954) 326–327, https://doi.org/10.1007/BF00644489.
[50] H. Ruppersberg, W. Speicher, Density and compressibility of liquid Li-Pb alloys, Z. Naturforsch. 31a (1976) 47–52, https://doi.org/10.1515/zna-1976-0106.
[51] K.J. Mysels, The maximum bubble pressure method of measuring surface tension, revisited, Colloid. Surface. 43 (1990) 241–262, https://doi.org/10.1016/0166-6622(90)80291-B.
[52] I. Korobenikov, R. Endo, S. Seethraman, O. Volkova, Density of liquid manganese measured using the maximum bubble pressure method, Metall. Mater. Trans. B 52 (2021) 571–575, https://doi.org/10.1007/s11663-020-02044-y.
[53] P. Nikolopoulos, B. Schulz, Density, thermal expansion of stainless steel and interfacial properties of UO_2 -stainless steel above 1690 K, J. Nuc, Mat. 82 (1979) 172–178, https://doi.org/10.1016/0022-3115(79)90050-3.

[54] B.B. Alchagirov, Thermal properties of promising tritium reproducing materials and coolants of the liquid metal blanket of fusion reactor: lead-lithium eutectics, Perspekt, Materials 6 (2005) 35.
[55] S. Stankus, S.V. Kairulin, Density and phase diagram of the magnesium-lead system in the region of Mg_2Pb intermetallic compound, Thermochemica Acta 474 (2008) 52–56, https://doi.org/10.1016/j.tca.2008.05.011.
[56] V.Ya Prokhorenko, A.I. Kondyr, I.P. Pazdrii, Investigation of Structural Stability and Physicomechanical Properties of Eutectic in the Solid and Liquid Phases: A Report on Research Work, State Registration no. 01880053572, Lvov Polytechnical Inst, 1988.
[57] V.Ya Prokhorenko, A.I. Kondyr, I.P. Pazdrii, Investigation of Structural Stability and Physicomechanical Properties of Eutectic in the Solid and Liquid Phases: A Report on Research Work, State Registration no. 01880053572, Lvov Polytechnical Inst, 1990.
[58] S.V. Stankus, R.A. Kairulin, A.G. Mozgovoi, An experimental investigation of the density and thermal expansion of Advanced materials and heat-transfer agents of liquid–metal systems of fusion reactor: lead-lithium eutectic, High Temp. 44 (2006) 829–837, https://doi.org/10.1007/s10740-006-0100-5.
[59] R.A. Kairulin, R.N. Abdullaev, S.V. Stankus, Volumetric properties of lithium–lead melts, Int. J. Thermophys. 38 (2017) 23, https://doi.org/10.1007/s10765-016-2165-7.
[60] H.S. Carslaw, Conduction Fo Heat in Solids, second ed., Oxford science publications, 1959.
[61] A. Sh Agazhanov, R.N. Abdullaev, D.A. Samoshkin, S.V. Stankus, Thermal conductivity and thermal diffusivity of Li-Pb eutectic in the temperature range of 293-1273 K, Fusion Eng. Des. 152 (2020) 111456, https://doi.org/10.1016/j.fusengdes.2020.111456.
[62] Y.S. Touloukian, R.W. Powell, C.Y. Ho, M.C. Nicolaou, Thermal Diffusivity, Vol. 10 of Thermophysical Properties of Matter, FI/Plenum, New York-Washington, 1973. https://apps.dtic.mil/sti/citations/ADA129113.
[63] W.J. Parker, R.J. Jenkins, C.P. Butler, G.L. Abbott, Flash method of determining thermal diffusivity, heat capacity, and thermal conductivity, J. Appl. Phys. 32 (1961) 1679–1684, https://doi.org/10.1063/1.1728417.
[64] S.V. Stankus, I.V. Savchenko, Laser flash method for measurement of liquid metals heat transfer coeffcients, Thermophys. Aeromechanics 16 (2009) 585–592, https://doi.org/10.1134/S0869864309040076.
[65] I.V. Savchenko, S.V. Stankus, A.S. Agazhanov, Heat transfer coeffcients of liquid indium in the temperature range 470-1275 K, Thermophys. Aeromechanics 17 (2010) 121–125, https://doi.org/10.1134/S0869864310010142.
[66] I.V. Savchenko, S.V. Stankus, A.S. Agazhanov, Measurement of the thermal conductivity and diffusivity of molten lead in the interval 601-1000 K, Energy 115 (2013) 83–87, https://doi.org/10.1007/s10512-013-9753-4.
[67] A.S. Agazhanov, R.N. Abdullaev, D.A. Samoshkin, S.V. Stankus, Thermal conductivity of lithium, sodium and potassium in the liquid state, Phys. Chem. Liq. 58 (2020) 760–768, https://doi.org/10.1080/00319104.2019.1636377.
[68] J.G. Hust, L.L. Sparks, Lorenz rations of technically important metals and alloys, in: NBS Technical Note, vol. 634, US Department of Commerce Publication, 1973. https://archive.org/details/lorenzratiosofte634hust.
[69] V.T. Nguyen, J.E. Enderby, The electronic structure of lithium-based liquid semiconducting alloys, Phil. Mag. 35 (4) (1977) 1013–1019, https://doi.org/10.1080/14786437708232641.
[70] J.A. Meijer, W. Geertsma, W. van der Lugt, Electrical resistivities of liquid alkali-lead and alkali-indium alloys, J. Phys. F Met. Phys. 15 (1985) 899–910, https://doi.org/10.1088/0305-4608/15/4/014.
[71] P. Hubberstey, M.G. Barker, T. Sample, An electrical resistivity monitor for the detection of composition changes in Pb-17Li, Fusion Eng. Des. 14 (1991) 227–233, https://doi.org/10.1016/0920-3796(91)90006-C.
[72] C.C. Addison, G.K. Creffield, P. Hubberstey, R.J. Pulham, Electrical resistivity of solutions of barium in liquid sodium, J. Chem. Soc. (Lond.) A (1971) 1393–1396, https://doi.org/10.1039/J19710001393.
[73] P. Favuzza, R. Marinari, Test results and upgrade design of Resistivity Meter for on-line N monitoring, IFMIF-DONES Report, ENS-5.4.5.1-T6-22-N1, https://idm.euro-fusion.org/default.aspx?uid=2MRG69, 2020.
[74] R. Franz, Ueber die Wärme-Leitungsfähigkeit der Metalle, Ann. Phys. 165 (8) (1853) 497–531, https://doi.org/10.1002/andp.18531650802.
[75] A. Sommerfeld, Zur Elektronentheorie der Metalle, Naturwissenschaften 15 (1927) 825–832, https://doi.org/10.1007/BF01505083.
[76] U. Mizutani, Introduction to the Electron Theory of Metals, CAMBRIDGE UNIVERSITY PRESS, 2001, https://doi.org/10.1017/CBO9780511612626. ISBN 9780511612626.
[77] T.M. Tritt, Thermal Conductivity: Theory, Properties, and Applications, Plenum Publishers, New York, 2004. ISBN 978-0-387-26017-4, https://link.springer.com/book/10.1007/b136496.
[78] J.M. Ziman, Electrons and phonons: the theory of transport phenomena in solids, in: Oxford Classic Texts in the Physical Sciences, vol. 1, Oxford Academic, Oxford, Sept. 2007, https://doi.org/10.1093/acprof:oso/9780198507796.001.0001, 2001; online edn,.
[79] B. Giordanengo, N. Benazzi, J. Vinckel, J.G. Gasser, L. Roubi, Thermal conductivity of liquid metals and metallic alloys, J. Non-Cryst. Solids 250–252 (1999) 377–383, https://doi.org/10.1016/S0022-3093(99)00268-9.
[80] H.U. Borgestedt, C. Guminski, IUPAC-NIST solubility data series. 75. Nonmetals in liquid alkali metals, J. Phys. Chem. Ref. Data 30 (4) (2001) 835–1158, https://doi.org/10.1063/1.1391426.
[81] E.M. Larsen, M.S. Ortman, K.E. Plute, Comments on the Hydrogen Solubility Data for Liquid Lead, Lithium, and Lithium-Lead Alloys and Review of a Tritium-Solubility Model for Lithium-Lead Alloys, Wisconsin Univ., Madison (USA), 1981. Dept. of Nuclear Engineering UWFDM-415, https://www.osti.gov/biblio/6256868.
[82] A.I. Demidov, A.G. Morachevskii, L.N. Gerasimenko, Thermodynamic properties of liquid lithium-lead alloys, Sov. Electrochem. 9 (1973) 813–814.
[83] S.P. Yatsenko, E.A. Saltykova, Thermodynamic properties of liquid lithium-lead alloys, Russ. J. Phys. Chem. 50 (1976) 1278.
[84] H.R. Ihle, The activity of lithium, and the solubility of deuterium. Proc. Tenth Symp. Fusion, Pergamon Press, New York, 1979, pp. 639–644.
[85] R. Schumacher, A. Weiss, Hydrogen solubility in the liquid alloys lithium-indium, lithium-lead, and lithium-tin, Ber. Bunsenges. Phys. Chem. 94 (1990) 684–691, https://doi.org/10.1002/bbpc.19900940612.
[86] M.G. Frohberg, S. Anik, Thermodynamic relations between component activities and gas solubilities in binary metallic systems, Ber. Bunsenges. Phys. Chem. 89 (1985) 130–134, https://doi.org/10.1002/bbpc.19850890210.
[87] F. Priester, R. Größle, N. Bekris, I. Cristescu, A new facility for the measurement of the Sieverts'-constant for PbLi with tritium, Fusion Eng. Des. 191 (2023) 113568, https://doi.org/10.1016/j.fusengdes.2023.113568.
[88] F. Reiter, Solubility and diffusivity of hydrogen isotopes in liquid Pb-17Li, Fusion Eng. Des. 14 (1991) 207–211, https://doi.org/10.1016/0920-3796(91)90003-9.
[89] H. Katsuta, H. Iwamoto, H. Ohno, Hydrogen solubility in liquid $Li_{17}Pb_{83}$, J. Nucl. Mater. 133&134 (1985) 167–170, https://doi.org/10.1016/0022-3115(85)90127-8.
[90] P. Fauvet, J. Sannier, Hydrogen behaviour in liquid 17Li83Pb alloy, J. Nucl. Mater. 155–157 (1988) 516–519, https://doi.org/10.1016/0022-3115(88)90301-7.
[91] H. Feurstein, H. Gräbner, S. Horn, J. Oschinski, Behavior of deuterium and rare gases in loops with molten Pb-17Li thermal convection, Fusion Eng. Des. 14 (1991) 261–271, https://doi.org/10.1016/0920-3796(91)90010-N.
[92] A. Aiello, A. Ciampichetti, G. Beneamati, Determination of hydrogen solubility in lead lithium using sole device, Fusion Eng. Des. 81 (2006) 639–644, https://doi.org/10.1016/j.fusengdes.2005.06.364.
[93] Y. Edao, H. Noguchi, S. Fukada, Experiments of hydrogen isotope permeation, diffusion and dissolution in Li-Pb, J. Nucl. Mater. 417 (2011) 723–726, https://doi.org/10.1016/j.jnucmat.2010.12.126.
[94] H. Okitsu, Y. Edao, M. Okada, S. Fukada, Analysis of diffusion and dissolution of two-component hydrogen (H + D) in lead lithium, Fusion Eng. Des. 87 (2012) 1324–1328, https://doi.org/10.1016/j.fusengdes.2012.03.004.
[95] S. Kumar, A. Tirpude, N. Krishnamurthy, Studies on the solubility of hydrogen in molten $Pb_{83}Li_{17}$ eutectic alloy, I. J. Hydr, Energy 38 (2013) 6002–6007, https://doi.org/10.1016/j.ijhydene.2013.03.033.
[96] G. Alberro, I. Peñalva, A. Sarrionandia-Ibarra, F. Legarda, G.A. Esteban, Experimental determination of solubility values for hydrogen isotopes in eutectic Pb-Li, Fusion Eng. Des. 98–99 (2015) 1919–1923, https://doi.org/10.1016/j.fusengdes.2015.05.060.
[97] L. Candido, C. Alberghi, Tbm – test execution on HyPer-QuarCh and data elaboration 2020-2021, WPBB Deliverable BB-6.3.7-T005-D002. https://idm.euro-fusion.org/default.aspx?uid=2P3V8K, 2021.
[98] H. Feurstein, H. Gräbner, J. Oschinski, S. Horn, Evaporation of lead and lithium from molten Pb-17Li - transport of aerosols, Fusion Eng. Des. 17 (1991) 203–207, https://doi.org/10.1016/0920-3796(91)90058-X.
[99] L. Candido, C. Alberghi, A. Antonelli, S. Bassini, M. Piccioni, S. Storai, R. Testoni, M. Utili, M. Zucchetti, HyPer-QuarCh II: a laboratory-scale device for hydrogen isotopes permeation experiments, Fusion Eng. Des. 172 (2021) 112920, https://doi.org/10.1016/j.fusengdes.2021.112920.